HHS Public Access

Author manuscript

Brain Struct Funct. Author manuscript; available in PMC 2017 July 01.

Published in final edited form as:

Brain Struct Funct. 2016 July ; 221(6): 2937–2962. doi:10.1007/s00429-015-1081-0.

Organization of connections between the amygdala, medial prefrontal cortex, and lateral hypothalamus: a single and double retrograde tracing study in rats

Christina J. Reppucci[1] and **Gorica D. Petrovich**[1]

[1] Department of Psychology, Boston College, 344 McGuinn Hall, 140 Commonwealth Avenue, Chestnut Hill, MA 02467, USA

Abstract

The amygdala and medial prefrontal cortex (mPFC) are highly interconnected telencephalic areas critical for cognitive processes, including associative learning and decision making. Both structures strongly innervate the lateral hypothalamus (LHA), an important component of the networks underlying the control of feeding and other motivated behaviors. The amygdala–prefrontal–lateral hypothalamic system is therefore well positioned to exert cognitive control over behavior. However, the organization of this system is not well defined, particularly the topography of specific circuitries between distinct cell groups within these complex, heterogeneous regions. This study used two retrograde tracers to map the connections from the amygdala (central and basolateral area nuclei) and mPFC to the LHA in detail, and to determine whether amygdalar pathways to the mPFC and to LHA originate from the same or different neurons. One tracer was placed into a distinct mPFC area (dorsal anterior cingulate, prelimbic, infralimbic, or rostromedial orbital), and the other into dorsal or ventral LHA. We report that the central nucleus and basolateral area of the amygdala send projections to distinct LHA regions, dorsal and ventral, respectively. The basolateral area, but not central nucleus, also sends substantial projections to the mPFC, topographically organized rostrocaudal to dorsoventral. The entire mPFC, in turn, projects to the LHA, providing a separate route for potential amygdalar influence following mPFC processing. Nearly all amygdalar projections to the mPFC and to the LHA originated from different neurons suggesting amygdala and amygdala–mPFC processing influence the LHA independently, and the balance of these parallel pathways ultimately controls motivated behaviors.

Keywords

Amygdala; Prefrontal cortex; Hypothalamus; Behavior; Motivation; Feeding

Gorica D. Petrovich gorica.petrovich@bc.edu.

Compliance with ethical standards

Conflict of interest The authors declare that they have no conflict of interest.

Ethical approval All applicable international, national, and institutional guidelines for the care and use of animals were followed. All procedures performed in this study involving animals were in accordance with the ethical standards of the Boston College Institutional Animal Care and Use Committee.

Introduction

The amygdala and medial prefrontal cortex (mPFC) are highly interconnected telencephalic areas critical for cognitive processes, including associative learning and decision making (e.g., Cassell and Wright 1986; Euston et al. 2012; Krettek and Price 1977b; McDonald 1998; Seymour and Dolan 2008). Each structure strongly innervates the lateral hypothalamus (LHA) (e.g., Hurley et al. 1991; Kita and Oomura 1982; Petrovich et al. 2001; Yoshida et al. 2006), which is an important component of the networks underlying the control of feeding and other motivated behaviors (Elmquist et al. 1999; Swanson 2005). The amygdala–prefrontal–lateral hypothalamic system is therefore well positioned to exert cognitive control over behavior, and recent studies on feeding behavior support this notion. Intact amygdala, mPFC, and their connections with the LHA are required for the control of food intake by learned environmental cues, independent of physiological state (Holland et al. 2002; Petrovich et al. 2005, 2007a, b, 2009). In addition, stimulation of the mPFC μ-opioid (Mena et al. 2011) or dopamine (Land et al. 2014) systems elicits robust feeding in sated animals, and these effects depend on activation of the LHA (Mena et al. 2013) and amygdala (Land et al. 2014), respectively.

The connectional organization of this functional amygdala–prefrontal–lateral hypothalamic system is not well defined. In particular, the topography of specific subsystems between these three large forebrain regions is unknown. This is especially critical given that the amygdala, mPFC and LHA are complex heterogeneous regions comprised of distinct cell groups that mediate different functions (e.g., Ashwell and Ito 2014; Burgos-Robles et al. 2013; Cole et al. 2013; Heidbreder and Groenewegen 2003; Knapska et al. 2012; Maeng and Shors 2013; Martinez et al. 2013; Mendoza et al. 2014; Senn et al. 2014; Swanson and Petrovich 1998). Prior work, with anterograde or retrograde tracing methods, has identified direct pathways from the amygdala to the mPFC and to the LHA, as well as direct pathways from the mPFC to the LHA (e.g., Hoover and Vertes 2007; Hurley et al. 1991; Kita and Oomura 1982; Krettek and Price 1977b, 1978; Ono et al. 1985; Sesack et al. 1989), including the mid-rostrocaudal (tuberal) LHA region which contains orexigenic neuropeptides (Broberger et al. 1998; Hahn 2010; Swanson et al. 2005). This pattern of connections suggests that in addition to direct pathways, the amygdala could also influence the LHA indirectly through the mPFC, following mPFC processing (Gabbott et al. 2012). Nevertheless, a comprehensive analysis of the entire system has not been conducted. In addition, no study to date has examined whether amygdalar pathways to the mPFC and to the LHA originate in common or distinct cell groups, and characterizing how these connections are organized is important for determining whether the amygdala influences the mPFC and LHA simultaneously or independently.

The present study had two aims. The first aim was to map the organization of connections between the amygdala, mPFC, and LHA (tuberal region, see below), in detail. The second aim was to determine whether the pathways from the amygdala to the mPFC and LHA originate in the same or different groups of neurons. We employed a dual retrograde tract tracing design, which involved placements of different retrograde tracers into the mPFC and LHA. To accomplish the first aim, we analyzed single tracer distribution within the amygdala after retrograde transport from the mPFC and LHA, and distribution within the

mPFC after retrograde transport from the LHA. To accomplish the second aim, we analyzed the distribution of both tracers simultaneously within the amygdala. Within the amygdala, we analyzed two large areas, critical for associative learning and subsequent control of behavior [including the control of feeding by learned cues (Holland et al. 2002; Petrovich et al. 2009) and fear conditioning (e.g., Anglada-Figueroa and Quirk 2005; Goosens and Maren 2001; Ledoux 2012; Maren et al. 1996)]: the basolateral area [consisting of the basolateral (BLA), basomedial (BMA), and lateral nuclei (LA)], and the central nucleus (CEA). These two areas are structurally distinct, and based on developmental, cytoarchitectonic, and connectional features are considered highly differentiated parts of the cortex (basolateral area) or striatum (CEA) (McDonald 2003; Swanson and Petrovich 1998). Within the mPFC, we focused on four regions defined based on their distinct cytoarchitecture and connections (Heidbreder and Groenewegen 2003; Swanson 2004): the anterior cingulate area (ACAd), the prelimbic area (PL), the infralimbic area (ILA), and a rostromedial orbital region (comprised of the medial (ORBm) and ventrolateral (ORBvl) parts of the orbital area). Finally, because of our interest in feeding behavior, the mid-rostrocaudal (tuberal) LHA, which receives dense amygdalar and mPFC inputs and has the highest concentration of the orexigenic peptides, was divided into two targets: the dorsal, which contains these orexigenic peptides, and the ventral which lacks these peptides.

Materials and methods

Subjects

Forty experimentally naïve, male Long–Evans rats approximately 2 months of age (Charles River Laboratories, Portage, MI) were individually housed, maintained on a 12-h light/dark cycle, and had access to food and water ad libitum. Upon arrival, subjects were allowed 1 week to acclimate to the colony room, during which time they were handled daily. All housing and experimental procedures were in compliance with the National Institutes of Health *Guidelines for Care and Use of Laboratory Animals*, and approved by the Boston College Institutional Animal Care and Use Committee.

Surgical procedure

Animals were briefly anesthetized with isoflurane (5 %; Baxter Healthcare Corporation, Deerfield, IL, USA), then deeply anesthetized with an intramuscular injection of a mixture (1 ml/kg body weight) of ketamine (50 mg/mL; Fort Dodge Animal Health, Fort Dodge, Iowa) and xylazine (10 mg/mL; LLOYD Laboratories, Shenandoah, IA, USA). While under anesthesia, animals received two stereotaxically placed iontophoretic injections of retrograde tracers in the right hemisphere: one into the mPFC and the other into the LHA. Injection placements of 3 % Fluoro-Gold (FG; Fluorochrome, LLC, Denver, CO, USA) dissolved in 0.9 % saline, and 2 % Cholera Toxin B Subunit (CTB; 104; List Biological Laboratories, Inc., Campbell, CA, USA) dissolved in deionized water were counterbalanced for location across subjects. Each tracer was delivered through a glass micropipette (~50 μm tip diameter) by applying a positive current (5 μA, 5 s on/off intervals) for 10 min. This method allows for precise placement of the tracers with little damage to surrounding tissue and minimal risk of uptake from fibers of passage (Lanciego and Wouterlood 2011).

Histological procedures

Twelve to fifteen days following surgery, rats were briefly anesthetized with isoflurane, and then deeply anesthetized with an intraperitoneal injection of tribromoethanol (375 mg/kg; Sigma-Aldrich, St. Louis, MO, USA). Rats were then transcardially perfused with 0.9 % saline followed by 4 % paraformaldehyde in 0.1 M borate buffer. Brains were extracted and post-fixed overnight in the same fixative containing 12 % sucrose, and then rapidly frozen in hexanes cooled in dry ice and stored at −80 °C. Brains were sliced in 30 μm coronal sections using a sliding microtome and were collected into four adjacent series. Three tissue series were collected into a 0.02 M potassium phosphate-buffered saline (KPBS) solution. One was mounted on gelatin-coated slides and Nissl stained with thionin for identification of cytoarchitectonic borders (Simmons and Swanson 1993), and the other two series were processed immediately for immunohistochemical detection of each retrograde tracer (single-label). The fourth tissue series was collected into a tray containing a cryoprotectant solution (0.025 M sodium phosphate buffer with 30 % ethylene glycol and 20 % glycerol), and stored at −20 °C for later processing of combined detection of both tracers (double label).

Single-label immunohistochemistry—One series of tissue was stained for detection of FG. Free-floating sections were incubated in a blocking solution for 1 h at room temperature to minimize nonspecific antibody binding. The blocking solution contained KPBS, 0.3 % Triton X-100 (Sigma-Aldrich, St. Louis, MO, USA), 2 % normal goat serum (S-1000; Vector Laboratories, Burlingame, CA, USA), and 10 % non-fat milk (M-0841; LabS-cientific, Livingston, NJ, USA). After blocking, the tissue was incubated with the primary antibody, anti-FG raised in rabbit (1:20,000; AB153; Millipore, Billerica, MA, USA) in the blocking solution for 72 h at 4 °C. The tissue was rinsed with KPBS and then incubated with the secondary antibody, biotinylated goat anti-rabbit IgG (1:500; BA-1000; Vector Laboratories, Burlingame, CA, USA) in the blocking solution for 45 min. Subsequently, the tissue was rinsed with KPBS and then reacted with avidin–biotin complex (PK-6100; Vector Laboratories, Burlingame, CA, USA) for 45 min. After rinsing with KPBS, the tissue was incubated in a diaminobenzidine solution (SK-4100; Vector Laboratories, Burlingame, CA, USA) for 1 min with constant manual agitation to produce a color reaction.

A second series of tissue was stained for detection of CTB. The processing procedure was identical to that described above, except for the following differences. The normal serum used was from horse (S-2000; BA-9500; Vector Laboratories, Burlingame, CA, USA), the primary antibody was anti-CTB raised in goat (1:5000; 703; List Biological Laboratories, Inc., Campbell, CA, USA), and the secondary antibody was biotinylated horse anti-goat IgG (BA-9500; Vector Laboratories, Burlingame, CA, USA).

After processing, tissue sections were mounted onto SuperFrost Plus slides (Fisher Scientific, Pittsburgh, PA, USA), dried overnight at 45 °C, dehydrated through alcohols, cleared in xylenes, and coverslipped with DPX (13512; Electron Microscopy Sciences, Hatfield, PA, USA).

Double-label immunohistochemistry—For simultaneous visualization of both tracers, one series of brain tissue ($n = 4$) underwent fluorescent double-label immunohistochemical processing. Tissue was rinsed from the cryoprotectant storage solution with several washes in KPBS, and then incubated for 72 h at 4 °C in a blocking solution [KPBS containing 0.3 % Triton X-100, 2 % normal donkey serum (017-000-001; Jackson ImmunoRe-search, West Grove, PA, USA)], with both primary antibodies: anti-FG (1:10,000) and anti-CTB (1:5000). After rinses in KPBS, tissue was incubated for 1 h in the dark in the blocking solution containing the secondary antibodies: Alexa 488 anti-rabbit (1:200; A21206; Invitrogen, Carlsbad, CA, USA) and Alexa 546 anti-goat (1:200; A11056; Invitrogen, Carlsbad, CA, USA), both raised in donkey serum. Following rinses in KPBS, tissue was mounted in semidarkness onto slides (SuperFrost Plus), dried, coverslipped with Vectashield HardSet Mounting Medium with DAPI (H-1500; Vector Labs, Burlingame, CA, USA), and stored at 4 °C until analysis.

Image acquisition and analysis

Single-label detection—The analysis was conducted with an Olympus BX51 light microscope with attached Olympus DP72 camera, using DP2-BSW software (Olympus America Inc, Center Valley, PA, USA). Images of the areas with tracer deposits and the adjacent Nissl-stained tissue were acquired at 4×. To determine the location and extent of the tracer deposits, neuroanatomical borders were drawn onto the Nissl-stained image and then transposed to the adjacent immunohistochemically stained image using ImageJ software (NIH). These injection sites were then drawn on computerized versions of the standard rat brain atlas drawings (Swanson 2004) using illustration software (Adobe Illustrator CS5.5). Based on this analysis, well-defined and localized injections were identified and retrogradely labeled neurons were analyzed in those brains. Retrograde labeling was analyzed within the amygdala regions of interest (basolateral area and CEA) for all injection sites in the mPFC and LHA. In addition, retrograde labeling was analyzed within the mPFC for each LHA injection site. The LHA was examined for retrograde labeling following mPFC injections, but only very sparse labeling was observed, consistent with prior reports (Allen and Cechetto 1993; Goto et al. 2005; Hahn and Swanson 2012, 2015; Hoover and Vertes 2007; Saper 1985; Villalobos and Ferssiwi 1987), and thus this pathway was not systematically analyzed. Tracer-labeled neuron mapping was conducted from images acquired at 10× using ImageJ, confirming labeling at 20× and cytoarchitectonic borders (Nissl) at 4×, as needed. The locations of labeled neurons were plotted directly onto computerized versions of the standard drawings of the rat brain (Swanson 2004) using illustration software (Adobe Illustrator CS5.5). Retrograde labeling was not illustrated if fewer than five labeled neurons were observed. The pattern of retrograde labeling was not dependent on the specific retrograde tracer used; FG and CTB injections in similar regions produced indistinguishable patterns. The brains with less localized injection sites were also systematically examined; patterns of labeling were compared to the plots from the ideal injections to verify topographical patterns of labeling, and these brains were also inspected as potential candidates for double-label analysis (see below).

The parcellation and nomenclature of the rat brain followed Swanson (2004), except for the following differences. The term “basolateral area of the amygdala” refers to the area

comprised of the BLA (anterior and posterior parts; BLAa, BLAp), BMA (anterior and posterior parts; BMAa, BMAp), and LA. In comparison to another nomenclature scheme, the BLAa corresponds to the magnocellular and intermediate divisions of the basal nucleus, the BLAp to the parvicellular division of the basal nucleus, and the BMAa and BMAp partially overlap with the magnocellular and parvicellular divisions of the accessory basal nucleus (Pitkänen et al. 1997). Rostromedial ORB refers to the combined area of the ORBm and ORBvl as defined in the Swanson atlas (+5.20 to +4.20 from bregma), and it overlaps with the medial (MO) and ventral (VO) orbital areas defined by other groups (Floyd et al. 2001; Hoover and Vertes 2011; Krettek and Price 1977a; Van De Werd and Uylings 2008). LHA injections were grouped by their placement within dorsal or ventral LHA, which we defined here as the parts above (dorsal LHA) or below (ventral LHA) a horizontal line through mid fornix at mid-rostrocaudal (turberal) levels.

To better characterize the topography of amygdalar projections to the mPFC, the distribution of retrogradely labeled neurons in the amygdala was quantified in regard to cell group and rostrocaudal location for the plotted cases of ACAd, PL, and ILA injections (which varied in dorsoventral placement, but were located in a similar rostrocaudal location within the mPFC). Rostromedial ORB was not included in this analysis because injections were considerably more rostral than injections into the ACAd, PL, and ILA, and thus it would not be possible to determine if differences in the distribution of amygdalar inputs were due to its ventral location (compared to ACAd, PL) or rostral location (compared to ACAd, PL, ILA). For each case, representative images (tracer, Nissl) of the cell groups within the basolateral area of the amygdala were acquired at 10× for each level of the Swanson atlas (2004). Using ImageJ, regions of interests (ROIs) were created for each cell group (BLAa, BLAp, BMAp, and LA; there was no labeling in BMAa) on the Nissl-stained tissue images, and transposed to the images of the adjacent tracer-stained tissue. The number of retrogradely labeled neurons within each ROI was quantified using the ImageJ cell counter by a trained observer unaware of the injection site location. For each brain, the percent of labeled neurons located in each cell group was calculated (e.g., # of labeled neurons in BLAa/total # of labeled neurons in the entire basolateral area), as well as the percent of all labeled neurons in the rostral (atlas levels 26–28), mid (atlas levels 29–31), and caudal (atlas levels 32–34) basolateral area collapsed across cell groups (e.g., # of labeled neurons in rostral/total # of labeled neurons in the entire basolateral area).

Double-label detection—The analysis was conducted with a Zeiss Axioplan II fluorescence microscope (Carl Zeiss Microscopy GmbH, Jena, Germany) and attached Hamamatsu camera (Bridgewater, NJ, USA). Based on the findings from the single-label analysis, only the posterior basolateral amygdalar nuclei (BLAp, BMAp) contained retrograde labeling following both LHA and mPFC injections. Thus, to examine whether any neurons in the BLAp/BMAp region project to both the mPFC and LHA, four cases where inspection of both series of single-label tracer-stained tissue revealed labeling in this potential region of overlap were chosen for double-label processing and analysis. To examine potential double labeling, consecutive images were taken throughout atlas levels 30–34 (Swanson 2004).

Images were pseudocolored with red for CTB, green for FG, and blue for DAPI (nuclear counterstain); contrast was enhanced, and images were triple stacked using Improvision OpenLab (PerkinElmer, Waltham, MA, USA) imaging software. All analyses were conducted from the triple-merged images, however, single images were consulted as needed to confirm the cell and stain type. Neurons were deemed tracer-positive if they had robust cytoplasmic staining and a clearly visible DAPI-stained nucleus. For each image, the number of FG-positive, CTB-positive, and FG + CTB double-labeled neurons (visualized as yellow) were counted and summed across all images for each brain. The percent of all labeled neurons for each brain that was positive for both FG and CTB was then calculated (#double-labeled/[#FG + #CTB + #double-labeled]).

Results

Projections from the amygdala to the medial prefrontal cortex

The patterns of retrograde labeling in the amygdala were analyzed following injections into four discrete mPFC regions: ACAd, PL, ILA, and rostromedial ORB. Detailed descriptions of labeling patterns, and plots from representative injections are illustrated below. The densest labeling was observed after injections into the PL and ILA, while injections into rostromedial ORB resulted in the sparsest labeling. In all cases, retrograde labeling was restricted to the basolateral area of the amygdala (Fig. 1), while there was no labeling in the CEA. Most of the labeling was concentrated within BLAa and BLAp and adjacent ventral LA, while the ventral mPFC injections also produced substantial labeling in BMAp.

Projections to the anterior cingulate area—In two cases, the retrograde tracer injection was contained within the ACAd. The retrograde labeling pattern for one of these, #32 (Fig. 2a, c), is shown in detail. The pattern of labeling for another injection that was centered more caudally but still contained within ACAd (#52, Fig. 2b) was identical but less dense than #32.

The majority of labeled neurons following injections into the ACAd was contained within the BLAa (Fig. 1a) and BLAp. There were also some labeled neurons in the ventral portion of the LA, which formed a dorsal extension of the labeling in the BLA. Labeling was densest in the caudal third of the BLAa (atlas levels 28–29), an area that corresponds to the intermediate division of the basal nucleus (Savander et al. 1995), before quickly tapering off caudally. There were no retrogradely labeled neurons within the BMAa or BMAp.

Projections to the prelimbic area—In six cases, the retrograde tracer injection was predominately contained within the PL. The retrograde labeling pattern for one of these, #25 (Fig. 3a, c), is shown in detail because the tracer most completely filled the PL and its pattern of retrograde labeling was representative of other cases with injections into the PL (Fig. 3b). Five injections were used as comparisons; one was slightly smaller than the plotted example (#46), two were centered more rostrally and dorsally within the PL (#21 and #22), and two had dorsal spread into the ACAd (#20 and #33).

Injections into the PL produced the largest rostrocaudal spread of labeling in the amygdala of any mPFC injection. Similar to ACAd injections, the majority of labeled neurons were

within the BLAa and BLAp (Fig. 1b), but there were more labeled neurons across the rostrocaudal extent of LA. The densest labeling was in the caudal BLAa (atlas levels 29–30). There were no retrogradely labeled neurons within the BMAa, while there were some in the caudal half of BMAp, typically at the border with BLAp. We found a similar pattern for all the comparison injections. The pattern was nearly identical for #46. For the two cases that included dorsal spread into ACAd (#20 and #33), the density of labeling was similar to the plotted example, but the location was shifted slightly rostromedially such that the pattern of labeling was an intermediate to the plotted ACAd and PL injections. Back-labeling following the two most rostral PL injections (#21 and #22) was overall much less dense, and did not produce labeling in the most caudal third of the basolateral area (i.e., caudal LA, BLAp, BMAp).

Projections to the infralimbic area—In four cases, the retrograde tracer injection was contained within the ILA. The retrograde labeling pattern for one of these, #35 (Fig. 4a, c), is shown in detail because the injection site for this case most completely filled the entire ILA. Of the additional cases that were used for comparison analysis (Fig. 4b), two were smaller than the plotted case and did not include the most ventral third (#27) or half (#45) of ILA, while the third included the dorsoventral extent of ILA but was restricted to layers 5 and 6 (#36).

The majority of retrogradely labeled neurons after ILA injections were contained within the caudal basolateral area, specifically within the BLAp (Fig. 1c), where the densest labeling was medially within its rostral half. Labeling within the BLAa was restricted to its caudal half. There were no retrogradely labeled neurons within the BMAa, while there was moderate labeling within the BMAp, concentrated adjacent to the BLAp forming a continuum of labeled neurons across the BLAp/BMAp border. There were also scattered neurons throughout the rostrocaudal extent of the LA. The overall pattern was similar in the comparison injections. In cases where the injections were centered slightly more dorsal than the plotted example (#27 and #45), there was additional BLAa labeling, similar in location to that following injections into PL. The smallest ILA injection (#36) produced the same pattern of labeling, but less dense than the plotted example.

Projections to the rostromedial orbital area—In six cases, the retrograde tracer injection was concentrated within very rostral and ventral mPFC. The retrograde labeling analysis for one of these, #40 (Fig. 5a, c), is shown in detail because its injection site was nearly completely contained within the rostromedial ORB (ORBm and ORBvl), and its pattern of retrograde labeling was representative of patterns from other injections into this region (Fig. 5b). Of the additional five cases, one was similarly contained within the ORBm and ORBvl but was smaller in size (#51), and one was contained exclusively within the ORBvl (#43). Injections in the remaining three cases spread dorsally into rostral PL (#48, #50, #49).

Injections into the rostromedial ORB resulted in the sparsest amygdalar labeling of any mPFC area. The majority of retrogradely labeled neurons were located within the BLAa and adjacent rostral part of the BLAp, while very few labeled neurons were found in LA. This

pattern was consistent for all the comparison injections, except for the largest (#48) where labeling was more robust and continued further caudally, compared to the plotted case (#40).

Topography of amygdala projections to the medial prefrontal cortex

We observed no labeling within the CEA following tracer injections into any region of the mPFC. This finding demonstrates that the CEA does not send any direct projections to the mPFC. In contrast, we found substantial labeling within the basolateral area of the amygdala following retrograde tracer injections in the mPFC, and these connections were topographically organized. Specifically, the most dorsal mPFC tracer injection placement (ACAd) more heavily labeled rostral regions (BLAa), while the most ventral mPFC tracer injection placement (ILA) more heavily labeled caudal regions (BLAp and BMAp), and mid dorsoventral placed mPFC injections (PL) produced an intermediate pattern of labeling (Fig. 6). A quantitative analysis of the distribution of labeling confirmed this pattern (Table 1). Thus, we found a rostrocaudal to dorsoventral topography in amygdala projections to the mPFC.

Projections from the amygdala and medial prefrontal cortex to the lateral hypothalamus

Retrograde tracer injections into the dorsal LHA produced strikingly different patterns of labeling in the amygdala and mPFC compared to injections into the ventral LHA. Injections into dorsal LHA primarily labeled the CEA (Fig. 7a) and the entire dorsoventral and rostrocaudal extent of the mPFC (Fig. 8a). In contrast, injections into ventral LHA primarily labeled regions of the basolateral area of the amygdala (Fig. 7d), and a select ventrocaudal portion of the mPFC (Fig. 8b).

Projections to the dorsal LHA—In seven cases, the retrograde tracer injection was predominately located within the dorsal LHA. The retrograde labeling pattern for one of these, #23 (Fig. 9a, c, d), is shown in detail because the injection was centered above fornix, it most completely included the entire dorsal portion of the LHA, and the pattern of labeling was representative of other injections into this region (Fig. 9b). Other injections were centered more dorsally with some spread into the zona incerta (#37 and #55), or were placed medial to fornix (#26, #28, #40 and #41).

Within the amygdala, the majority of labeled neurons following injections into the dorsal LHA was concentrated within the CEA. Sparser labeling was present in the BMAa and the most rostral portion of the BMAp (Fig. 9c). In contrast, there was no significant labeling in the LA, BLAa, or BLAp following dorsal LHA injections (Fig. 7c). Within the CEA, there were labeled neurons in all three subdivisions (lateral part (CEAl), medial part (CEAm), and capsular part (CEAc)); the division with the overall greatest number of labeled neurons was the CEAm, though the single densest group of labeled neurons was within CEAl (Figs. 7a, 8c). This dense group of labeled neurons was completely contained within the CEAl rostrally (atlas level 26), and formed a continuum with CEAm caudally. This distinct labeling was also present in other cases with dorsal LHA injections (#26, #28, #40 and #41), except for the two most dorsal cases (#37 and #55), suggesting that the CEA most strongly projects to areas bordering fornix.

Retrograde tracer injections into the dorsal LHA also resulted in extensive labeling of the mPFC (Figs. 8a, 9d), throughout its entire rostocaudal extent. This labeling was almost entirely contained within layer 5, although there was some labeling in layer 6 caudally. Most of the labeling was concentrated within the PL and ILA, but extended dorsally through the ACAd. Rostrally, labeling extended laterally from ORBm, across the ORBvl and the lateral part of the orbital area (ORBl). Caudally, there were labeled neurons in layer 6 of the ventral part of the orbital area (ORBv). The labeling pattern was similar in the comparison injections, with minor variations in density. There was less labeling in rostral mPFC (atlas levels 4–6) for most of the cases, while in two cases (#37 and #55) there was more labeling in caudal ILA (atlas level 11).

Projections to the ventral LHA—In six cases, the retrograde tracer injection was contained within ventral LHA. The retrograde labeling pattern for one of these, #21 (Fig. 10a, c, d), is shown in detail because the tracer injection most completely filled the entire ventral LHA, and its pattern of labeling was representative of other cases following injections into this region (Fig. 10b). Among comparison injections, one (#24) was very similar in size and placement to the represented case, two were located ventrolaterally and mostly within the tuberal nucleus (TU; #51 and #53), and two were smaller, located medially, and primarily contained within the ventral zone of the juxtaventromedial region of the LHA (LHAjvv; #29 and #52).

Following retrograde tracer injection into the ventral LHA, the majority of labeled neurons in the amygdala were within three distinct groups within the basolateral area: the medial half of the BMAa, the dorsal half of the BMAp, and a small ventrolateral group in the LA (Figs. 7d, 10c). The dense labeling within the BMAa was located medially and extended across its rostrocaudal extent. The labeling in the BMAp was concentrated dorsally, and tapered off laterally in the BLAp. Caudally, labeled neurons in the BMAp and BLAp, together with posterior amygdalar nucleus (labeling not shown), formed a continuous group below and parallel to the stria terminalis. The third group was in the caudal third of the LA, specifically within its ventrolateral corner. There was no labeling in the BLAa. Sparser labeling was observed throughout the CEA, mostly in CEAc but also in CEAl and CEAm (Fig. 7b). Overall labeling in the CEA was light to moderate in the plotted example, but was much lighter in the comparison injections which did not include the region bordering fornix (#29, #51, #52, #53), suggesting that the perifornical region of the LHA is preferentially the target of CEA inputs.

This pattern of labeling was replicated in the case where the injection was nearly identical (#24), except for slightly more labeling in the CEA, which may be attributed to injection's spread dorsally and medially around fornix. In the comparison injections, labeling in the BMAa was lighter than the plotted example; however, labeling in other basolateral area regions depended on injection placement. In the cases where the injection was located more medially (#29 and #52), the pattern of labeling in BMAp, BLAp, and LA was similar to the plotted example. The two cases restricted to the most ventrolateral edge of the ventral LHA (#51 and #53) had more restricted BMAp labeling (only labeling caudally, adjacent to posterior amygdalar nucleus) and there was no labeling in LA.

In contrast to dorsal LHA injections that produced extensive mPFC labeling, ventral LHA injections produced very restricted labeling within the ventrocaudal region, specifically in the ventral PL, ILA and ORBv (Figs. 8b, 10d). Similar to the pattern after dorsal LHA injections, labeling was mainly contained within layer 5, but included some labeling in layer 6. All comparison cases had a similar pattern of mPFC labeling, with minor variations in density.

Parallel amygdala pathways to the medial prefrontal cortex and lateral hypothalamus

The single-label analysis of retrograde labeling patterns, described above, revealed that amygdalar projections to the mPFC and LHA arise primarily in separate nuclei. Specifically, the BLA most strongly innervates the mPFC, while the BMA and CEA most strongly innervate the LHA. Rostrally, there was no potential for overlap as the populations of neurons projecting to the mPFC and LHA were topographically distinct (i.e., BLAa to mPFC; BMAa and CEA to LHA). Caudally, however, labeling from injections into the mPFC and LHA was present in adjacent nuclei, BLAp and BMAp, particularly across their border region (Fig. 11a).

Examination of the double-labeled tissue confirmed that separate populations of neurons within the basolateral area of the amygdala innervate the mPFC and LHA. There was very little overlap between the two populations of neurons rostrally, as expected from the analysis of single-labeled tissue. Even caudally, where the two populations of retrograde tracer-labeled neurons were intermixed, the occurrence of double-labeled neurons was very seldom (Fig. 11b). Indeed, only 1.31 ± 0.29 % (mean ± SEM, $n = 4$) of all tracer-labeled neurons were double-labeled, indicating they projected to both targets. Thus, more than 98 % of all labeled neurons projected to only one target, thereby confirming that amygdala pathways to the mPFC and LHA arise primarily in separate populations of neurons.

Discussion

This study examined the organization of connections between the amygdala, mPFC, and LHA with dual retrograde tract tracing and immunohistochemical techniques. Within the amygdala, we analyzed the topography of pathways from the CEA and basolateral area to the mPFC and LHA in detail. These areas are cytoarchitectonically heterogeneous, and we characterized distinct pathways from their different nuclei that form multiple subsystems within the amygdala–prefrontal–lateral hypothalamic network. We found that both the CEA and the basolateral area send direct projections to the LHA, while only the basolateral area also sends direct projections to the mPFC. Within the LHA, the CEA and basolateral area innervate different regions, the dorsal and ventral LHA, respectively. In addition, the strongest pathways from the basolateral area to the mPFC and LHA were from different nuclei, the BLA and BMA, respectively, and nearly all (>98 %) of these projections originated from different neurons. To our knowledge, this was the first study to directly examine whether the same or different amygdalar neurons project to the mPFC and LHA. Thus, we found evidence for multiple, direct pathways from the CEA and basolateral area to the LHA, and separate pathways from the BLA to areas of the mPFC that send direct projections to the LHA (Fig. 12).

Comparisons with prior studies

Amygdalar projections to the mPFC—The current study found extensive direct projections to the mPFC from the basolateral area of the amygdala, but not from the CEA, in accordance with prior observations (Hoover and Vertes 2007; McDonald 1991; Swanson and Petrovich 1998). The primary sources of the afferents to the mPFC were the BLAa and BLAp, and adjacent regions, dorsally the LA and ventromedially the BMAp (Fig. 1). These pathways are topographically organized (Fig. 6; Table 1); the BLAa more heavily projects to the dorsal mPFC (e.g., ACAd, dorsal PL) compared to the caudal nuclei, the BLAp and BMAp, which more heavily project to the ventral mPFC (e.g., ventral PL, ILA). This detailed topography adds to prior retrograde tracing work which had shown a topographical organization of projections from the basolateral area of the amygdala to the entire prefrontal cortex (McDonald 1987). The rostrocaudal to dorsoventral topography of amygdala to mPFC projections had been observed in prior work, however, that study more strongly emphasized a rostrocaudal to rostrocaudal topography, especially for ILA inputs (Hoover and Vertes 2007). In the present study, we also observed a similar topography for amygdalar inputs to the PL, in that our more rostrally placed injections into PL (Fig. 3b) only produced labeling in the most rostral basolateral area (BLAa and very rostral BLAp), and injections into very rostral mPFC, the rostromedial orbital area, resulted in labeling restricted mainly to the BLAa (Fig. 5).

We found the most substantial retrograde labeling within the amygdala after injections into either the PL or ILA. The largest rostrocaudal extent of labeling was observed following injections into PL, which is in agreement with prior work (Hoover and Vertes 2007). Although the rostrocaudal spread of amygdalar retrograde labeling was greater following PL injections, the overall amount of labeling was similarly strong following injections into the PL and ILA, which was consistent with prior reports (Hoover and Vertes 2007). In comparison, the amount of retrograde labeling after ACAd injection was much less, which was also previously reported (Hoover and Vertes 2007).

Our findings are in general agreement with prior anterograde tracing work that found extensive innervation of the mPFC by the amygdala. In early studies, injections were large and therefore preclude direct comparisons with specific nuclei in the current study. Injections that encompassed the LA, BLAa, and BLAp produced dense labeling within the PL and ILA, and the highest density within layer 5 (Krettek and Price 1977b). That study reported denser projections to the mPFC from BLAp compared to the BLAa; however, the reduced amount of labeling after BLAa injections may be explained by considerable spread into the CEA (Krettek and Price 1977b). A later study (Kita and Kitai 1990) with a more sensitive tracer (Lanciego and Wouterlood 2011) also reported strong innervation of the mPFC (with particularly dense terminations in layer 5) after caudal (i.e., BLAp, BMAp, and caudal LA) but not after rostral (i.e., BLAa, rostral LA) injections into the basolateral area. In contrast, we found that the BLAa and BLAp projected equally strongly to the mPFC, albeit to different regions (i.e., dorsal and ventral mPFC, respectively; Table 1). In agreement with the rostrocaudal amygdala to dorsoventral mPFC topography we observed, a previous study found that the BMAp moderately innervated layer 5 of the ventral mPFC (e.g., ILA, ventral PL), but did not innervate the dorsal mPFC (e.g., dorsal PL, ACAd)

(Petrovich et al. 1996). In the present study, we did not observe any labeled neurons in the BMAa after retrograde tracer placement into any mPFC location, in agreement with very sparse innervation restricted to the superficial layers of the ILA from the BMAa (Petrovich et al. 1996).

Amygdalar projections to the LHA—Connections from the amygdala to the hypothalamus are well known (Petrovich et al. 2001), and prior anterograde studies determined that the most substantial input to the LHA is from the CEA, while the basolateral area more strongly innervates the medial zone nuclei (Petrovich et al. 2001). Similarly, a retrograde tracing study found that the greatest contribution to the LHA was the CEA, but also noted labeling in the BMA, LA, and BLA (Ono et al. 1985). Extending prior work, here we found that the CEA and basolateral area nuclei most strongly projected to different parts of the LHA, the dorsal and ventral LHA, respectively (Fig. 7). Specifically, all subdivisions of the CEA were labeled after retrograde injections into the dorsal LHA with the greatest contribution from CEAm and CEAl, while the medial half of the BMAa, the dorsal half of the BMAp and laterally adjacent BLAp, and a small ventro-lateral group in the LA were labeled after injections into the ventral LHA.

Based on prior anterograde work, the amygdala densely innervates three distinct fields across rostrocaudal LHA (Petrovich et al. 2001), which may explain why some previous studies with single retrograde tracer deposits in LHA did not produce labeling in the CEA (Cassell et al. 1986; Kita and Oomura 1982). The first field spans the dorsal LHA and is strongly innervated by the CEAm and CEAc (Petrovich et al. 2001), and in agreement we observed similar patterns in the current study after injections into the dorsal LHA. The second field is a caudolateral portion of the LHA, and is strongly innervated by the CEAm and CEAc and lightly by the BMAa and BLAp (Petrovich et al. 2001). However, neither the dorsal nor ventral LHA injections in the present study were centered in that region. The third field is ventromedial LHA (including the TU), which is moderately innervated by the BLAp and BMAp (Petrovich et al. 1996, 2001); our ventral LHA injections were placed within this field, and produced labeling consistent with this pattern.

The present study found substantial retrograde labeling within the CEA and basolateral area nuclei, but after tracer injections into different parts of the LHA. This is consistent with prior observations that the CEA and BLA send parallel fibers to the LHA (Krettek and Price 1978), and that the CEA sends substantial projections into the dorsal LHA (Ono et al. 1985; Petrovich et al. 2001; Yoshida et al. 2006). Retrograde labeling in the CEA was dense after injections into the dorsal LHA and light to moderate following injections into the ventral LHA, but only when injections included the regions directly adjacent to fornix, suggesting the CEA preferentially targets the perifornical region (for CEA projections to far lateral regions see: Petrovich et al. 2001). Light labeling following ventral LHA injections is consistent with prior work that found sparse labeling after discrete injections into the dorsal and ventral zones of the juxtaventromedial LHA (LHAjvd, LHAjvv) (Hahn and Swanson 2015) and no labeling after injections into TU (Toth et al. 2010). Our findings that the rostral half of the CEAl has much stronger projections to the LHA than the caudal CEAl is consistent with a previous study that did not find significant labeling within the LHA from the caudal CEAl (Petrovich and Swanson 1997). Light to moderately dense projections from

the basolateral area of the amygdala to the LHA have also been reported previously (Ono et al. 1985; Petrovich et al. 2001), and in general agreement we found substantial labeling in distinct nuclei within this area. Specifically, the BMAa projects to both dorsal and ventral LHA, while caudal regions (BMAp, BLAp, LA) project to only the ventral LHA. Early anterograde work (Krettek and Price 1978) did not find LHA labeling after injections restricted to the BMA. However, consistent with the current results, a later anterograde tracing study (Petrovich et al. 1996) with a more sensitive tracer (Lanciego and Wouterlood 2011) and a recent study with retrograde injections into discrete ventral LHA cell groups (LHAjvd or LHAjvv) (Hahn and Swanson 2015), showed moderate to dense input from the BMAa and BMAp.

The LHA is a highly differentiated region (Swanson 2004) and it is important to determine which specific cell groups receive inputs from the CEA, and particularly from the dense cluster of neurons we identified (across CEAm/CEAl; Figs. 7a, 8c) after tracer injections into the dorsal LHA. Recent work has started to systematically examine inputs and outputs of discrete LHA cell groups (Hahn and Swanson 2010, 2012, 2015). Of particular interest are two regions, supraformical (LHAs) and juxtadorsomedial (LHAjd), which are included within the dorsal LHA of the present study. Retrograde tracer injections confined to LHAs resulted in the labeling of a dense group of neurons in the CEAl, and sparse labeling in CEAm, CEAc, BMAa, and caudal BLAp (Hahn and Swanson 2010). In contrast, retrograde tracer deposits restricted to the LHAjd did not label the CEAl, and resulted in low labeling of the CEAm, CEAc, and all regions of the basolateral area of the amygdala (Hahn and Swanson 2012). Thus, the dense labeling within the CEA we observed after dorsal LHA retrograde tracer injections is, at least in part, due to specific projections to the LHAs.

The specific phenotype of CEA neurons projecting to LHA has not been characterized; however, CEA neurons are nearly exclusively GABAergic (Swanson and Petrovich 1998), and additionally express various neuropeptides, especially within the CEAl (e.g., Cassell et al. 1986; Day et al. 1999; Haubensak et al. 2010; Li et al. 2013; Marchant et al. 2007; Roberts et al. 1982; Wray and Hoffman 1983). Based on topographical distribution, the CEAm/CEAl group of neurons that strongly projects to the LHA may contain enkephalin (Cassell et al. 1986; Day et al. 1999; Wray and Hoffman 1983). A subpopulation of CEAl neurons expresses protein kinase C-δ (PKCδ), a substantial proportion of which coexpress enkephalin (Haubensak et al. 2010). Interestingly, recent work found that the PKCδ-positive neurons are critical for fear (Haubensak et al. 2010), and for the inhibition of feeding (Cai et al. 2014). Nevertheless, other neuropeptides are also densely expressed within portions of this area (e.g., somatostatin, corticotropin-releasing hormone, neurotensin), and CEA to LHA pathways are likely heterogeneous in terms of neuropeptide content. In that regard, neurons in the LHA are responsive to many of the neuropeptides and the neurotransmitter expressed by the CEA (Stanley et al. 2011; Tsujino and Sakurai 2009).

Within the LHA, the targets of CEA inputs include neurons that express two orexigenic neuropeptides: melanin-concentrating hormone (MCH) and orexin/hypocretin (Broberger et al. 1998; de Lecea et al. 1998; Griffond and Risold 2009; Hahn 2010; Nahon et al. 1989; Sakurai et al. 1998; Swanson et al. 2005). Anterograde tract tracing combined with orexin detection showed that the CEA (specifically the CEAl) innervates a substantial proportion of

orexin neurons in the LHA, especially within the perifornical region, which somewhat overlaps with our dorsal LHA and includes LHAs (Yoshida et al. 2006). Additional detailed analyses revealed that GABAergic CEA terminals innervate orexin and MCH neurons (Nakamura et al. 2009). Interestingly, the BMAa—the only other amygdalar nucleus that sends substantial input to the dorsal LHA (current study)—also innervates MCH neurons, and these projections are glutamatergic (Niu et al. 2012). It remains to be determined whether BMAa neurons also innervate orexin neurons.

mPFC projections to the LHA—The current study found that the entire rostrocaudal and dorsoventral extent of the mPFC projects to the dorsal LHA, while only a restricted ventrocaudal region of the mPFC (i.e., ILA and adjacent PL and ORBv) also projects to the ventral LHA. This is consistent with other studies that reported labeling along the dorsoventral extent of the mPFC (Gabbott et al. 2005; Kita and Oomura 1982), and laterally across the orbital regions (Gabbott et al. 2005) after retrograde tracer injections that included both dorsal and ventral LHA, and studies with deposits restricted to cell groups ventral to fornix that reported labeling in caudal PL, ILA, and ORBv (Hahn and Swanson 2015; Toth et al. 2010). Also consistent with prior work, most of the labeled neurons were in layer 5, with moderate labeling in layer 6 (Gabbott et al. 2005).

Current findings also align with previous observations with anterograde tract tracing (Floyd et al. 2001; Hoover and Vertes 2011). These studies have shown stronger projections to the perifornical and lateral regions of the LHA from the ventral compared to the dorsal mPFC (Hoover and Vertes 2011; Hurley et al. 1991; Sesack et al. 1989; Takagishi and Chiba 1991; Vertes 2004). Similarly, we found that the ventral mPFC had more projections to the LHA, compared to the dorsal mPFC. In general agreement with a previously demonstrated rostrocaudal gradient of projections from the mPFC (specifically from PL) to the LHA (Floyd et al. 2001), we observed more labeled neurons in rostral than caudal PL following retrograde injections into dorsal LHA. Taken together, prior and current findings suggest that the density of mPFC inputs to the LHA increases along two axes to create a dorsorostral to ventrocaudal gradient of light to dense innervation.

Recent, high-resolution analyses of discrete dorsal LHA regions provide additional topographical specificity to the patterns of mPFC to LHA projections. Retrograde tracer deposits in regions medial to (LHAjd) or directly above (LHAs) fornix moderately labeled the entire medial wall of the mPFC and lightly labeled the rostromedial orbital area (Hahn and Swanson 2010, 2012), while deposits lateral to fornix in a region that corresponds to LHAd (Swanson 2004) resulted in labeling that was restricted to the ILA (Hurley et al. 1991). Together with the present report, these findings suggest that ACAd, PL, and rostromedial orbital regions project specifically to the LHAjd and LHAs, while the ILA projects to the entire dorsal area of LHA. Finally, the mPFC inputs to the LHA include the area with neurons that express the peptides MCH and orexin. Anterograde tracing combined with orexin detection confirmed that ILA neurons directly innervate orexin neurons across the entire orexin field (Yoshida et al. 2006). Whether projections from other mPFC areas also innervate orexin neurons, and whether any mPFC neurons innervate MCH neurons, remains unknown.

Functional significance

It is instructive to review the organization of the amygdala–prefrontal–lateral hypothalamic system delineated in the current study within larger structural and functional frameworks. The two large amygdalar areas examined are differentiated parts of the striatum or cortex that belong to different functional systems—autonomic (CEA), main olfactory (BMAa, BMAp, BLAp), or frontotemporal (BLAa, LA) (Swanson and Petrovich 1998). In agreement with this organization, the most substantial output to the LHA was from the striatal, autonomic system (CEA) and the nuclei that belong to the main olfactory cortex (BMAa, BMAp, BLAp). The nuclei that belong to the frontotemporal cortex (BLAa and LA) did not send direct input to the LHA (except for a small, ventrolateral group of neurons within the LA), and they also do not send pathways to the bed nuclei of the stria terminalis (BST) (Dong et al. 2001a), which would provide an indirect route to the LHA (Dong et al. 2000, 2001b; Dong and Swanson 2003, 2004a, b, 2006a, b, c). A reverse pattern was observed for amygdalar pathways to the mPFC. The cortical (except BMAa), but not striatal (CEA), nuclei sent topographically organized projections to the mPFC, and the strongest inputs were from the BLAa, BLAp, and BMAp, while the LA input was more limited.

Nevertheless, the LA sends substantial projections to another cortical region, the hippocampal formation (HF), which provides access to the hypothalamus (Canteras and Swanson 1992; Cenquizca and Swanson 2006; Petrovich et al. 2001; Risold and Swanson 1996). Interestingly, the only part of the LA that has direct projections to the LHA (current study)—the ventrolateral region—does not project to the HF (Petrovich et al. 2001). This topography suggests parallel LA pathways reach the LHA directly and indirectly via the HF, as different LA regions send direct pathways to the LHA and the HF. In contrast, the BLAa does not send any direct projections to the HF (Petrovich et al. 2001). The two frontotemporal cortical nuclei, therefore, preferentially innervate either the mPFC or the HF. This dichotomy is also reflected in their outputs to the striatum. Neither sends direct projections to the CEA (except for a limited input to the capsular part, from LA) (Pitkänen et al. 1997; Swanson and Petrovich 1998); instead they substantially innervate other parts of the striatum. Similar to its widespread innervation of the mPFC, the BLAa sends widespread output to the striatum, including the nucleus accumbens and large portions of the caudoputamen not innervated by other parts of the amygdala (Kita and Kitai 1990). The LA, on the other hand, most substantially projects to the nucleus accumbens (Kita and Kitai 1990).

The connectional patterns described in the current study also agree with the organization of cerebral hemisphere, defined by Larry Swanson, that controls motivated behaviors through a triple descending projection—cortical, striatal, and pallidal (Swanson 2000, 2005). Here, we found that the LHA receives converging striatal (CEA) and cortical (BMA, BLA, mPFC) inputs, which are topographically organized (dorsal LHA: CEA, BMAa, entire mPFC; ventral LHA: BMAa, BMAp, BLAp, ILA). The third (pallidal) descending component, from the BST, has been defined anatomically (Dong et al. 2000, 2001a, b; Dong and Swanson 2003, 2004a, b, 2006a, b, c), and was recently functionally tested for the control of feeding (Jennings et al. 2013).

The present study found that different amygdalar neurons send direct projections to the mPFC and LHA, and thus parallel pathways, from different amygdalar subsystems, provide direct and indirect (via mPFC) inputs to the LHA. This framework suggests the amygdala influences the mPFC and LHA independently. Similar organization has been shown for amygdalar projections to the mediodorsal thalamus (MD) and mPFC (a target of the MD) (McDonald 1987). Parallel BLA pathways (originating mainly from different neurons) to the mPFC and ventral hippocampus were also recently reported (Senn et al. 2014). In contrast, many BLA (and adjacent BMA and LA) neurons send collaterals to simultaneously innervate the PFC and striatum (McDonald 1991).

Nearly all projections from the BLAa to mPFC arise from principal pyramidal neurons (McDonald 1992). Quantitative ultrastructural analyses of these BLA projections have shown that a vast majority (>95 %) of terminals synapse onto glutamatergic mPFC neurons in layers 2 and 5, but they also terminate (~5 %) onto inhibitory interneurons (Gabbott et al. 2006). This pattern of connections suggests the BLA could monosynaptically innervate mPFC output neurons and therefore influence their targets, including the LHA, as was recently demonstrated for layer 5 mPFC neurons which project to the spinal cord (Gabbott et al. 2012). Even though most BLA inputs synapse onto pyramidal mPFC neurons, and fewer directly innervate interneurons (Gabbott et al. 2006), electrical stimulation of BLA neurons can inhibit mPFC neuronal firing through monosynaptic (as well as polysynaptic) pathways (Dilgen et al. 2013; Perez-Jaranay and Vives 1991). Thus, BLA inputs could guide mPFC outputs through excitation or inhibition of pyramidal neurons.

Consistent with structural evidence, BLA inputs have been shown to influence mPFC during aversive- and reward-driven associative learning and subsequent behaviors, either through activation of pyramidal mPFC neurons or through inhibitory mechanisms. Pyramidal mPFC (PL, ILA) neurons which receive BLA (mostly BLAp) input showed increased activity (spiking and bursting) in response to a cue (odor) that predicts footshocks, but not to a control cue, at post-conditioning tests as well as during acquisition, while activity in mPFC neurons that were not responsive to BLA stimulation was unchanged (Laviolette et al. 2005). Furthermore, BLA inactivation significantly reduced the firing rate of pyramidal PL neurons in response to a conditioned fear cue (tone) and during conditioned lever pressing for food (Sotres-Bayon et al. 2012). Interestingly, the PL and ILA were differentially activated during the expression and extinction of conditioned fear (Sierra-Mercado et al. 2011), and correspondingly, the BLA neurons projecting to the PL were activated in response to an aversively conditioned stimulus (CS) while those projecting to the ILA were activated in response to an extinguished CS (Senn et al. 2014). Similarly, the BLAa was suggested to guide mPFC activity during the acquisition of cue–food associations, because its recruitment preceded that of the mPFC and BLAa–mPFC pathways (specifically PL) were activated during this learning (Cole et al. 2013, 2015; Keefer et al. 2014).

In accordance with BLA influence via inhibitory interneurons, spontaneous mPFC firing (specifically in rostral PL) was suppressed during presentations of an aversive-conditioned cue, and this suppression was eliminated with BLA lesions (Garcia et al. 1999). Other work has shown that GABA, but not glutamate, transmission in the mPFC increased due to activation of inhibitory interneurons when rats were placed in a cocaine-associated

environment, and that this inhibitory transmission could be blocked by basolateral area inactivation prior to context re-exposure (Chefer et al. 2011). Similarly, inactivation of the BLA–mPFC pathway via optogenetic inhibition of BLA terminals in PL inhibited cue-induced reinstatement of drug-seeking behavior (Stefanik and Kalivas 2013).

Thus, the BLA can control both the activation (Sotres-Bayon et al. 2012) and suppression (Garcia et al. 1999) of mPFC neurons in response to conditioned stimuli (appetitive and aversive). Importantly, separate populations of pyramidal mPFC neurons exhibited profiles of either monosynaptic excitation or suppression of baseline firing following BLA stimulation, and these two populations were under differential control of the dopamine system (Floresco and Tse 2007). Given that multiple, topographically organized pathways arise from different parts of the BLA and send pathways to different mPFC areas, it is likely that these two neuronal populations are parts of different BLA–mPFC subsystems. Characterizing the precise subsystems is essential given the heterogeneity of the amygdala and mPFC (Heidbreder and Groenewegen 2003; Swanson and Petrovich 1998). These caveats in regard to comparisons across functional studies and inconsistencies in nomenclature, unfortunately, are a much broader concern.

Sensory and associative processing within the BLA–mPFC system could, in turn, control feeding and other motivated behaviors through mPFC–hypothalamic connections. For example, stimulation of μ-opioid- (Mena et al. 2011, 2013) or dopamine D1- (Land et al. 2014) receptor containing mPFC neurons has been shown to drive food consumption. Within the hypothalamus, sites of their action include the dorsal (perifornical) LHA and orexin neurons. The effects of mPFC μ-opioid-elicited feeding were blocked by antagonism of NMDA glutamate receptors in the dorsal (perifornical) LHA (Mena et al. 2013), and stimulation of the mPFC μ-opioid system, in the absence food intake, recruited orexin and other neurons within the dorsomedial LHA (Mena et al. 2013). In addition, D1-receptor containing mPFC neurons were shown to sparsely innervate the LHA (Land et al. 2014).

The LHA, especially the dorsal (perifornical) area, which contains orexin and MCH neurons, has been proposed to integrate cognitive and environmental influences with physiological drives underlying the motivation to eat (e.g., Berthoud and Münzberg 2011; Petrovich 2013). For example, MCH and orexin have been implicated in feeding driven by learned food cues in the absence of hunger (Petrovich et al. 2012; Sherwood et al. 2015). Central orexin administration increases intake and motivation (breakpoint in progressive ratio responding) for palatable food, while peripheral administration of an orexin antagonist blocks these effects (Borgland et al. 2009; Cason and Aston-Jones 2013, 2014; Choi et al. 2010; Clegg et al. 2002; Nair et al. 2008). Orexin neurons are recruited by environments and cues that predict food (and other rewards) (Choi et al. 2010; Harris et al. 2005; Petrovich et al. 2012) as well as during the acquisition of cue–food associations (Cole et al. 2015). The BLA–mPFC system, can therefore access LHA feeding regulatory mechanisms as well as other motivational systems (e.g., Arvanitogiannis et al. 2000; Wise 1974).

In conclusion, here, we defined topographically organized connections for amygdalar influence on the lateral hypothalamus via direct and mPFC routes. Precisely, delineated organization of anatomical connections is an essential framework upon which functional

studies can build (Khan 2013). We focused on the control of feeding behavior, but the BLA–mPFC system could ultimately provide access for cognitive processing influence on hypothalamic circuitries underlying other motivated behaviors (Swanson 2000, 2005). The amygdala–prefrontal–hypothalamic network function is adaptive and necessary for survival, but also susceptible to potential dysregulation (Likhtik and Paz 2015; Petrovich 2013). For example, environmental learned signals engaging the BLA–mPFC systems can override internal homeostatic signals regulating feeding behavior (Petrovich 2013). More broadly, disruptions of this circuitry, particularly of the BLA–mPFC system, can result in maladaptive learning (Likhtik and Paz 2015), and thus suboptimal expression of motivated behaviors.

Acknowledgments

We thank Meghana Kuthyar and Heather Mayer for technical assistance. This research was supported in part by National Institute of Health grant DK085721 to G.D.P.

Abbreviations

ACAd	Anterior cingulate area, dorsal part
ACAv	Anterior cingulate area, ventral part
BLA	Basolateral amygdalar nucleus
BLAa	Basolateral amygdalar nucleus, anterior part
BLAp	Basolateral amygdalar nucleus, posterior part
BMA	Basomedial amygdalar nucleus
BMAa	Basomedial amygdalar nucleus, anterior part
BMAp	Basomedial amygdalar nucleus, posterior part
CEA	Central amygdalar nucleus
CEAc	Central amygdalar nucleus, capsular part
CEAl	Central amygdalar nucleus, lateral part
CEAm	Central amygdalar nucleus, medial part
fx	Fornix
ILA	Infralimbic area
LA	Lateral amygdalar nucleus
LHA	Lateral hypothalamic area
LHAd	Lateral hypothalamic area, dorsal region
LHAjd	Lateral hypothalamic area, juxtadorsomedial region

LHAjvd	Lateral hypothalamic area, juxtaventromedial region, dorsal zone
LHAjvv	Lateral hypothalamic area, juxtaventromedial region, ventral zone
LHAs	Lateral hypothalamic area, suprafornical region
mPFC	Medial prefrontal cortex
ORB	Orbital area
ORBl	Orbital area, lateral part
ORBm	Orbital area, medial part
ORBv	Orbital area, ventral part
ORBvl	Orbital area, ventrolateral part
PL	Prelimbic area
TU	Tuberal nucleus

References

Allen GV, Cechetto DF. Functional and anatomical organization of cardiovascular pressor and depressor sites in the lateral hypothalamic area. II. Ascending projections. J Comp Neurol. 1993; 330:421–438. [PubMed: 7682225]

Anglada-Figueroa D, Quirk GJ. Lesions of the basal amygdala block expression of conditioned fear but not extinction. J Neurosci. 2005; 25:9680–9685. [PubMed: 16237172]

Arvanitogiannis A, Tzschentke TM, Riscaldino L, Wise RA, Shizgal P. Fos expression following self-stimulation of the medial prefrontal cortex. Behav Brain Res. 2000; 107:123–132. [PubMed: 10628736]

Ashwell R, Ito R. Excitotoxic lesions of the infralimbic, but not prelimbic cortex facilitate reversal of appetitive discriminative context conditioning: the role of the infralimbic cortex in context generalization. Front Behav Neurosci. 2014; 8:63. [PubMed: 24616678]

Berthoud HR, Münzberg H. The lateral hypothalamus as integrator of metabolic and environmental needs: from electrical self-stimulation to opto-genetics. Physiol Behav. 2011; 104:29–39. [PubMed: 21549732]

Borgland SL, et al. Orexin A/hypocretin-1 selectively promotes motivation for positive reinforcers. J Neurosci. 2009; 29:11215–11225. [PubMed: 19741128]

Broberger C, De Lecea L, Sutcliffe JG, Hokfelt T. Hypocretin/orexin- and melanin-concentrating hormone-expressing cells form distinct populations in the rodent lateral hypothalamus: relationship to the neuropeptide Y and agouti gene-related protein systems. J Comp Neurol. 1998; 402:460–474. [PubMed: 9862321]

Burgos-Robles A, Bravo-Rivera H, Quirk GJ. Prelimbic and infralimbic neurons signal distinct aspects of appetitive instrumental behavior. PLoS ONE. 2013; 8:e57575. [PubMed: 23460877]

Cai H, Haubensak W, Anthony TE, Anderson DJ. Central amygdala PKC-delta(+) neurons mediate the influence of multiple anorexigenic signals. Nat Neurosci. 2014; 17:1240–1248. [PubMed: 25064852]

Canteras NS, Swanson LW. Projections of the ventral subiculum to the amygdala, septum, and hypothalamus: a PHAL anterograde tract-tracing study in the rat. J Comp Neurol. 1992; 324:180–194. [PubMed: 1430328]

Cason AM, Aston-Jones G. Role of orexin/hypocretin in conditioned sucrose-seeking in rats. Psychopharmacology. 2013; 226:155–165. [PubMed: 23096770]

Cason AM, Aston-Jones G. Role of orexin/hypocretin in conditioned sucrose-seeking in female rats. Neuropharmacology. 2014; 86:97–102. [PubMed: 25036612]

Cassell MD, Wright DJ. Topography of projections from the medial prefrontal cortex to the amygdala in the rat. Brain Res Bull. 1986; 17:321–333. [PubMed: 2429740]

Cassell MD, Gray TS, Kiss JZ. Neuronal architecture in the rat central nucleus of the amygdala: a cytological, hodological, and immunocytochemical study. J Comp Neurol. 1986; 246:478–499. [PubMed: 2422231]

Cenquizca LA, Swanson LW. Analysis of direct hippocampal cortical field CA1 axonal projections to diencephalon in the rat. J Comp Neurol. 2006; 497:101–114. [PubMed: 16680763]

Chefer VI, Wang R, Shippenberg TS. Basolateral amygdala-driven augmentation of medial prefrontal cortex GABAergic neurotransmission in response to environmental stimuli associated with cocaine administration. Neuropsychopharmacology. 2011; 36:2018–2029. [PubMed: 21633339]

Choi DL, Davis JF, Fitzgerald ME, Benoit SC. The role of orexin-A in food motivation, reward-based feeding behavior and food-induced neuronal activation in rats. Neuroscience. 2010; 167:11–20. [PubMed: 20149847]

Clegg DJ, Air EL, Woods SC, Seeley RJ. Eating elicited by orexin-a, but not melanin-concentrating hormone, is opioid mediated. Endocrinology. 2002; 143:2995–3000. [PubMed: 12130565]

Cole S, Powell DJ, Petrovich GD. Differential recruitment of distinct amygdalar nuclei across appetitive associative learning. Learn Mem. 2013; 20:295–299. [PubMed: 23676201]

Cole S, Hobin MP, Petrovich GD. Appetitive associative learning recruits a distinct network with cortical, striatal, and hypothalamic regions. Neuroscience. 2015; 286:187–202. [PubMed: 25463526]

Day HE, Curran EJ, Watson SJ Jr, Akil H. Distinct neurochemical populations in the rat central nucleus of the amygdala and bed nucleus of the stria terminalis: evidence for their selective activation by interleukin-1beta. J Comp Neurol. 1999; 413:113–128. [PubMed: 10464374]

de Lecea L, et al. The hypocretins: hypothalamus-specific peptides with neuroexcitatory activity. Proc Natl Acad Sci USA. 1998; 95:322–327. [PubMed: 9419374]

Dilgen J, Tejeda HA, O'Donnell P. Amygdala inputs drive feedforward inhibition in the medial prefrontal cortex. J Neurophysiol. 2013; 110:221–229. [PubMed: 23657281]

Dong HW, Swanson LW. Projections from the rhomboid nucleus of the bed nuclei of the stria terminalis: implications for cerebral hemisphere regulation of ingestive behaviors. J Comp Neurol. 2003; 463:434–472. [PubMed: 12836178]

Dong HW, Swanson LW. Organization of axonal projections from the anterolateral area of the bed nuclei of the stria terminalis. J Comp Neurol. 2004a; 468:277–298. [PubMed: 14648685]

Dong HW, Swanson LW. Projections from bed nuclei of the stria terminalis, posterior division: implications for cerebral hemisphere regulation of defensive and reproductive behaviors. J Comp Neurol. 2004b; 471:396–433. [PubMed: 15022261]

Dong HW, Swanson LW. Projections from bed nuclei of the stria terminalis, anteromedial area: cerebral hemisphere integration of neuroendocrine, autonomic, and behavioral aspects of energy balance. J Comp Neurol. 2006a; 494:142–178. [PubMed: 16304685]

Dong HW, Swanson LW. Projections from bed nuclei of the stria terminalis, dorsomedial nucleus: implications for cerebral hemisphere integration of neuroendocrine, autonomic, and drinking responses. J Comp Neurol. 2006b; 494:75–107. [PubMed: 16304681]

Dong HW, Swanson LW. Projections from bed nuclei of the stria terminalis, magnocellular nucleus: implications for cerebral hemisphere regulation of micturition, defecation, and penile erection. J Comp Neurol. 2006c; 494:108–141. [PubMed: 16304682]

Dong HW, Petrovich GD, Swanson LW. Organization of projections from the juxtacapsular nucleus of the BST: a PHAL study in the rat. Brain Res. 2000; 859:1–14. [PubMed: 10720609]

Dong HW, Petrovich GD, Swanson LW. Topography of projections from amygdala to bed nuclei of the stria terminalis. Brain Res Rev. 2001a; 38:192–246. [PubMed: 11750933]

Dong HW, Petrovich GD, Watts AG, Swanson LW. Basic organization of projections from the oval and fusiform nuclei of the bed nuclei of the stria terminalis in adult rat brain. J Comp Neurol. 2001b; 436:430–455. [PubMed: 11447588]

Elmquist JK, Elias CF, Saper CB. From lesions to leptin: hypothalamic control of food intake and body weight. Neuron. 1999; 22:221–232. [PubMed: 10069329]

Euston DR, Gruber AJ, McNaughton BL. The role of medial prefrontal cortex in memory and decision making. Neuron. 2012; 76:1057–1070. [PubMed: 23259943]

Floresco SB, Tse MT. Dopaminergic regulation of inhibitory and excitatory transmission in the basolateral amygdala–pre-frontal cortical pathway. J Neurosci. 2007; 27:2045–2057. [PubMed: 17314300]

Floyd NS, Price JL, Ferry AT, Keay KA, Bandler R. Orbitomedial prefrontal cortical projections to hypothalamus in the rat. J Comp Neurol. 2001; 432:307–328. [PubMed: 11246210]

Gabbott PL, Warner TA, Jays PR, Salway P, Busby SJ. Prefrontal cortex in the rat: projections to subcortical autonomic, motor, and limbic centers. J Comp Neurol. 2005; 492:145–177. [PubMed: 16196030]

Gabbott PL, Warner TA, Busby SJ. Amygdala input monosynaptically innervates parvalbumin immunoreactive local circuit neurons in rat medial prefrontal cortex. Neuroscience. 2006; 139:1039–1048. [PubMed: 16527423]

Gabbott PL, Warner TA, Brown J, Salway P, Gabbott T, Busby S. Amygdala afferents monosynaptically innervate corticospinal neurones in rat medial prefrontal cortex (mPFC). J Comp Neurol. 2012; 520:2440–2458. [PubMed: 22247040]

Garcia R, Vouimba RM, Baudry M, Thompson RF. The amygdala modulates prefrontal cortex activity relative to conditioned fear. Nature. 1999; 402:294–296. [PubMed: 10580500]

Goosens KA, Maren S. Contextual and auditory fear conditioning are mediated by the lateral, basal, and central amygdaloid nuclei in rats. Learn Mem. 2001; 8:148–155. [PubMed: 11390634]

Goto M, Canteras NS, Burns G, Swanson LW. Projections from the subfornical region of the lateral hypothalamic area. J Comp Neurol. 2005; 493:412–438. [PubMed: 16261534]

Griffond B, Risold PY. MCH and feeding behavior-interaction with peptidic network. Peptides. 2009; 30:2045–2051. [PubMed: 19619600]

Hahn JD. Comparison of melanin-concentrating hormone and hypocretin/orexin peptide expression patterns in a current parceling scheme of the lateral hypothalamic zone. Neurosci Lett. 2010; 468:12–17. [PubMed: 19850103]

Hahn JD, Swanson LW. Distinct patterns of neuronal inputs and outputs of the juxtaparaventricular and suprafornical regions of the lateral hypothalamic area in the male rat. Brain Res Rev. 2010; 64:14–103. [PubMed: 20170674]

Hahn JD, Swanson LW. Connections of the lateral hypothalamic area juxtadorsomedial region in the male rat. J Comp Neurol. 2012; 520:1831–1890. [PubMed: 22488503]

Hahn JD, Swanson LW. Connections of the juxtaventromedial region of the lateral hypothalamic area in the male rat. Front Syst Neurosci. 2015; 9:66. [PubMed: 26074786]

Harris GC, Wimmer M, Aston-Jones G. A role for lateral hypothalamic orexin neurons in reward seeking. Nature. 2005; 437:556–559. [PubMed: 16100511]

Haubensak W, et al. Genetic dissection of an amygdala microcircuit that gates conditioned fear. Nature. 2010; 468:270–276. [PubMed: 21068836]

Heidbreder CA, Groenewegen HJ. The medial prefrontal cortex in the rat: evidence for a dorso-ventral distinction based upon functional and anatomical characteristics. Neurosci Biobehav Rev. 2003; 27:555–579. [PubMed: 14599436]

Holland PC, Petrovich GD, Gallagher M. The effects of amygdala lesions on conditioned stimulus-potentiated eating in rats. Physiol Behav. 2002; 76:117–129. [PubMed: 12175595]

Hoover WB, Vertes RP. Anatomical analysis of afferent projections to the medial prefrontal cortex in the rat. Brain Struct Funct. 2007; 212:149–179. [PubMed: 17717690]

Hoover WB, Vertes RP. Projections of the medial orbital and ventral orbital cortex in the rat. J Comp Neurol. 2011; 519:3766–3801. [PubMed: 21800317]

Hurley KM, Herbert H, Moga MM, Saper CB. Efferent projections of the infralimbic cortex of the rat. J Comp Neurol. 1991; 308:249–276. [PubMed: 1716270]

Jennings JH, Rizzi G, Stamatakis AM, Ung RL, Stuber GD. The inhibitory circuit architecture of the lateral hypothalamus orchestrates feeding. Science. 2013; 341:1517–1521. [PubMed: 24072922]

Keefer, SE.; Reppucci, CJ.; Mayer, HS.; Petrovich, GD. Program No. 650.11. 2014 Neuroscience Meeting Planner. Society for Neuroscience; Washington, DC: 2014. Plasticity within the basolateral amygdala pathways to the prelimbic cortex during Pavlovian appetitive conditioning.. (online)

Khan AM. Controlling feeding behavior by chemical or gene-directed targeting in the brain: what's so spatial about our methods? Front Neurosci. 2013; 7:182. [PubMed: 24385950]

Kita H, Kitai ST. Amygdaloid projections to the frontal cortex and the striatum in the rat. J Comp Neurol. 1990; 298:40–49. [PubMed: 1698828]

Kita H, Oomura Y. An HRP study of the afferent connections to rat lateral hypothalamic region. Brain Res Bull. 1982; 8:63–71. [PubMed: 6173104]

Knapska E, et al. Functional anatomy of neural circuits regulating fear and extinction. Proc Natl Acad Sci USA. 2012; 109:17093–17098. [PubMed: 23027931]

Krettek JE, Price JL. The cortical projections of the mediodorsal nucleus and adjacent thalamic nuclei in the rat. J Comp Neurol. 1977a; 171:157–191. [PubMed: 64477]

Krettek JE, Price JL. Projections from the amygdaloid complex to the cerebral cortex and thalamus in the rat and cat. J Comp Neurol. 1977b; 172:687–722. [PubMed: 838895]

Krettek JE, Price JL. Amygdaloid projections to subcortical structures within the basal forebrain and brainstem in the rat and cat. J Comp Neurol. 1978; 178:225–254. [PubMed: 627625]

Lanciego JL, Wouterlood FG. A half century of experimental neuroanatomical tracing. J Chem Neuroanat. 2011; 42:157–183. [PubMed: 21782932]

Land BB, et al. Medial prefrontal D1 dopamine neurons control food intake. Nat Neurosci. 2014; 17:248–253. [PubMed: 24441680]

Laviolette SR, Lipski WJ, Grace AA. A subpopulation of neurons in the medial prefrontal cortex encodes emotional learning with burst and frequency codes through a dopamine D4 receptor-dependent basolateral amygdala input. J Neurosci. 2005; 25:6066–6075. [PubMed: 15987936]

Ledoux J. Rethinking the emotional brain. Neuron. 2012; 73:653–676. [PubMed: 22365542]

Li H, Penzo MA, Taniguchi H, Kopec CD, Huang ZJ, Li B. Experience-dependent modification of a central amygdala fear circuit. Nat Neurosci. 2013; 16:332–339. [PubMed: 23354330]

Likhtik E, Paz R. Amygdala–prefrontal interactions in (mal)adaptive learning. Trends Neurosci. 2015; 38:158–166. [PubMed: 25583269]

Maeng LY, Shors TJ. The stressed female brain: neuronal activity in the prelimbic but not infralimbic region of the medial prefrontal cortex suppresses learning after acute stress. Front Neural Circuits. 2013; 7:198. [PubMed: 24391548]

Marchant NJ, Densmore VS, Osborne PB. Coexpression of prodynorphin and corticotrophin-releasing hormone in the rat central amygdala: evidence of two distinct endogenous opioid systems in the lateral division. J Comp Neurol. 2007; 504:702–715. [PubMed: 17722034]

Maren S, Aharonov G, Fanselow MS. Retrograde abolition of conditional fear after excitotoxic lesions in the basolateral amygdala of rats: absence of a temporal gradient. Behav Neurosci. 1996; 110:718–726. [PubMed: 8864263]

Martinez RC, et al. Active vs. reactive threat responding is associated with differential c-Fos expression in specific regions of amygdala and prefrontal cortex. Learn Mem. 2013; 20:446–452. [PubMed: 23869027]

McDonald AJ. Organization of amygdaloid projections to the mediodorsal thalamus and prefrontal cortex: a fluorescence retrograde transport study in the rat. J Comp Neurol. 1987; 262:46–58. [PubMed: 3624548]

McDonald AJ. Organization of amygdaloid projections to the prefrontal cortex and associated striatum in the rat. Neuroscience. 1991; 44:1–14. [PubMed: 1722886]

McDonald AJ. Projection neurons of the basolateral amygdala: a correlative Golgi and retrograde tract tracing study. Brain Res Bull. 1992; 28:179–185. [PubMed: 1375860]

McDonald AJ. Cortical pathways to the mammalian amygdala. Prog Neurobiol. 1998; 55:257–332. [PubMed: 9643556]

McDonald AJ. Is there an amygdala and how far does it extend? Ann NY Acad Sci. 2003; 985(1):1–21. [PubMed: 12724144]

Mena JD, Sadeghian K, Baldo BA. Induction of hyperphagia and carbohydrate intake by mu-opioid receptor stimulation in circumscribed regions of frontal cortex. J Neurosci. 2011; 31:3249–3260. [PubMed: 21368037]

Mena JD, Selleck RA, Baldo BA. Mu-opioid stimulation in rat prefrontal cortex engages hypothalamic orexin/hypocretin-containing neurons, and reveals dissociable roles of nucleus accumbens and hypothalamus in cortically driven feeding. J Neurosci. 2013; 33:18540–18552. [PubMed: 24259576]

Mendoza J, Sanio C, Chaudhri N. Inactivating the infralimbic but not prelimbic medial prefrontal cortex facilitates the extinction of appetitive Pavlovian conditioning in Long–Evans rats. Neurobiol Learn Mem. 2014; 118:198–208. [PubMed: 25543024]

Nahon JL, Presse F, Bittencourt JC, Sawchenko PE, Vale W. The rat melanin-concentrating hormone messenger ribonucleic acid encodes multiple putative neuropeptides coexpressed in the dorsolateral hypothalamus. Endocrinology. 1989; 125:2056–2065. [PubMed: 2477226]

Nair SG, Golden SA, Shaham Y. Differential effects of the hypocretin 1 receptor antagonist SB 334867 on high-fat food self-administration and reinstatement of food seeking in rats. Br J Pharmacol. 2008; 154:406–416. [PubMed: 18223663]

Nakamura S, Tsumori T, Yokota S, Oka T, Yasui Y. Amygdaloid axons innervate melanin-concentrating hormone- and orexin-containing neurons in the mouse lateral hypothalamus. Brain Res. 2009; 1278:66–74. [PubMed: 19414001]

Niu JG, Yokota S, Tsumori T, Oka T, Yasui Y. Projections from the anterior basomedial and anterior cortical amygdaloid nuclei to melanin-concentrating hormone-containing neurons in the lateral hypothalamus of the rat. Brain Res. 2012; 1479:31–43. [PubMed: 22902618]

Ono T, Luiten PGM, Nishijo H, Fukuda M, Nishino H. Topographic organization of projections from the amygdala to the hypothalamus of the rat. Neurosci Res. 1985; 2:221–238. [PubMed: 4022458]

Perez-Jaranay JM, Vives F. Electrophysiological study of the response of medial prefrontal cortex neurons to stimulation of the basolateral nucleus of the amygdala in the rat. Brain Res. 1991; 564:97–101. [PubMed: 1777825]

Petrovich GD. Forebrain networks and the control of feeding by environmental learned cues. Physiol Behav. 2013; 121:10–18. [PubMed: 23562305]

Petrovich GD, Swanson LW. Projections from the lateral part of the central amygdalar nucleus to the postulated fear conditioning circuit. Brain Res. 1997; 763:247–254. [PubMed: 9296566]

Petrovich GD, Risold PY, Swanson LW. Organization of projections from the basomedial nucleus of the amygdala: a PHAL study in the rat. J Comp Neurol. 1996; 374:387–420. [PubMed: 8906507]

Petrovich GD, Canteras NS, Swanson LW. Combinatorial amygdalar inputs to hippocampal domains and hypothalamic behavior systems. Brain Res Rev. 2001; 38:247–289. [PubMed: 11750934]

Petrovich GD, Holland PC, Gallagher M. Amygdalar and prefrontal pathways to the lateral hypothalamus are activated by a learned cue that stimulates eating. J Neurosci. 2005; 25:8295–8302. [PubMed: 16148237]

Petrovich GD, Ross CA, Gallagher M, Holland PC. Learned contextual cue potentiates eating in rats. Physiol Behav. 2007a; 90:362–367. [PubMed: 17078980]

Petrovich GD, Ross CA, Holland PC, Gallagher M. Medial prefrontal cortex is necessary for an appetitive contextual conditioned stimulus to promote eating in sated rats. J Neurosci. 2007b; 27:6436–6441. [PubMed: 17567804]

Petrovich GD, Ross CA, Mody P, Holland PC, Gallagher M. Central, but not basolateral, amygdala is critical for control of feeding by aversive learned cues. J Neurosci. 2009; 29:15205–15212. [PubMed: 19955373]

Petrovich GD, Hobin MP, Reppucci CJ. Selective Fos induction in hypothalamic orexin/hypocretin, but not melanin-concentrating hormone neurons, by a learned food-cue that stimulates feeding in sated rats. Neuroscience. 2012; 224:70–80. [PubMed: 22922124]

Pitkänen A, Savander V, LeDoux JE. Organization of intra-amygdaloid circuitries in the rat: an emerging framework for understanding functions of the amygdala. Trends Neurosci. 1997; 20:517–523. [PubMed: 9364666]

Risold PY, Swanson LW. Structural evidence for functional domains in the rat hippocampus. Science. 1996; 272:1484–1486. [PubMed: 8633241]

Roberts GW, Woodhams PL, Polak JM, Crow TJ. Distribution of neuropeptides in the limbic system of the rat: the amygdaloid complex. Neuroscience. 1982; 7:99–131. [PubMed: 6176906]

Sakurai T, et al. Orexins and orexin receptors: a family of hypothalamic neuropeptides and G protein-coupled receptors that regulate feeding behavior. Cell. 1998; 92:573–585. [PubMed: 9491897]

Saper CB. Organization of cerebral cortical afferent systems in the rat. II. Hypothalamocortical projections. J Comp Neurol. 1985; 237:21–46. [PubMed: 2995455]

Savander V, Go CG, LeDoux JE, Pitkänen A. Intrinsic connections of the rat amygdaloid complex: projections originating in the basal nucleus. J Comp Neurol. 1995; 361:345–368. [PubMed: 8543667]

Senn V, et al. Long-range connectivity defines behavioral specificity of amygdala neurons. Neuron. 2014; 81:428–437. [PubMed: 24462103]

Sesack SR, Deutch AY, Roth RH, Bunney BS. Topographical organization of the efferent projections of the medial prefrontal cortex in the rat: an anterograde tract-tracing study with *Phaseolus vulgaris* leucoagglutinin. J Comp Neurol. 1989; 290:213–242. [PubMed: 2592611]

Seymour B, Dolan R. Emotion, decision making, and the amygdala. Neuron. 2008; 58:662–671. [PubMed: 18549779]

Sherwood A, Holland PC, Adamantidis A, Johnson AW. Deletion of melanin concentrating hormone receptor-1 disrupts overeating in the presence of food cues. Physiol Behav. 2015 in press.

Sierra-Mercado D, Padilla-Coreano N, Quirk GJ. Dissociable roles of prelimbic and infralimbic cortices, ventral hippocampus, and basolateral amygdala in the expression and extinction of conditioned fear. Neuropsychopharmacology. 2011; 36:529–538. [PubMed: 20962768]

Simmons DM, Swanson LW. The Nissl stain. Neurosci Protoc. 050-12-01-07. 1993

Sotres-Bayon F, Sierra-Mercado D, Pardilla-Delgado E, Quirk GJ. Gating of fear in prelimbic cortex by hippocampal and amygdala inputs. Neuron. 2012; 76:804–812. [PubMed: 23177964]

Stanley BG, Urstadt KR, Charles JR, Kee T. Glutamate and GABA in lateral hypothalamic mechanisms controlling food intake. Physiol Behav. 2011; 104:40–46. [PubMed: 21550353]

Stefanik MT, Kalivas PW. Optogenetic dissection of basolateral amygdala projections during cue-induced reinstatement of cocaine seeking. Front Behav Neurosci. 2013; 7:213. [PubMed: 24399945]

Swanson LW. Cerebral hemisphere regulation of motivated behavior. Brain Res. 2000; 886:113–164. [PubMed: 11119693]

Swanson, LW. An atlas with printed and electronic templates for data, models, and schematics. 3rd rev. edn.. Elsevier, Academic Press; Amsterdam: 2004. Brain maps III: structure of the rat brain..

Swanson LW. Anatomy of the soul as reflected in the cerebral hemispheres: neural circuits underlying voluntary control of basic motivated behaviors. J Comp Neurol. 2005; 493:122–131. [PubMed: 16254987]

Swanson LW, Petrovich GD. What is the amygdala? Trends Neurosci. 1998; 21:323–331. [PubMed: 9720596]

Swanson LW, Sanchez-Watts G, Watts AG. Comparison of melanin-concentrating hormone and hypocretin/orexin mRNA expression patterns in a new parceling scheme of the lateral hypothalamic zone. Neurosci Lett. 2005; 387:80–84. [PubMed: 16084021]

Takagishi M, Chiba T. Efferent projections of the infralimbic (area 25) region of the medial prefrontal cortex in the rat: an anterograde tracer PHA-L study. Brain Res. 1991; 566:26–39. [PubMed: 1726062]

Toth M, Fuzesi T, Halasz J, Tulogdi A, Haller J. Neural inputs of the hypothalamic “aggression area” in the rat. Behav Brain Res. 2010; 215:7–20. [PubMed: 20685366]

Tsujino N, Sakurai T. Orexin/hypocretin: a neuropeptide at the interface of sleep, energy homeostasis, and reward system. Pharmacol Rev. 2009; 61:162–176. [PubMed: 19549926]

Van De Werd HJ, Uylings HB. The rat orbital and agranular insular prefrontal cortical areas: a cytoarchitectonic and chemoarchitectonic study. Brain Struct Funct. 2008; 212:387–401. [PubMed: 18183420]

Vertes RP. Differential projections of the infralimbic and prelimbic cortex in the rat. Synapse. 2004; 51:32–58. [PubMed: 14579424]

Villalobos J, Ferssiwi A. The differential ascending projections from the anterior, central and posterior regions of the lateral hypothalamic area: an autoradiographic study. Neurosci Lett. 1987; 81:89–94. [PubMed: 3696478]

Wise RA. Lateral hypothalamic electrical stimulation: does it make animals 'hungry'? Brain Res. 1974; 67:187–209. [PubMed: 4620218]

Wray S, Hoffman GE. Organization and interrelationship of neuropeptides in the central amygdaloid nucleus of the rat. Peptides. 1983; 4:525–541. [PubMed: 6196761]

Yoshida K, McCormack S, Espana RA, Crocker A, Scammell TE. Afferents to the orexin neurons of the rat brain. J Comp Neurol. 2006; 494:845–861. [PubMed: 16374809]

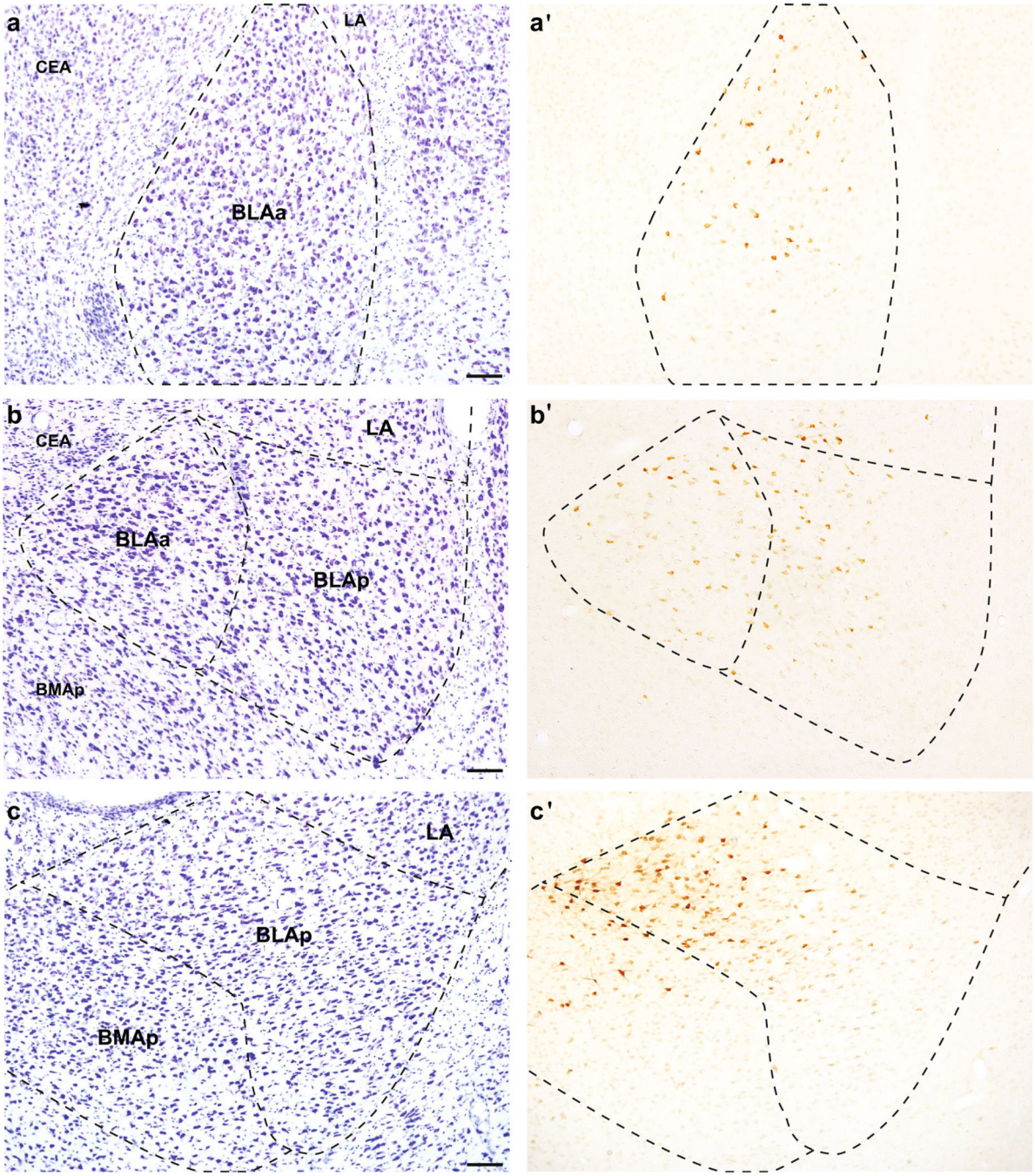

Fig. 1.

Representative images of retrograde tracer labeling in the basolateral area of the amygdala after tracer placement in the ACAd (**a′**; #32), PL (**b′**; #25), and ILA (**c′**; #35). **a–c** Adjacent Nissl-stained tissue. *Scale bars* 100 μm

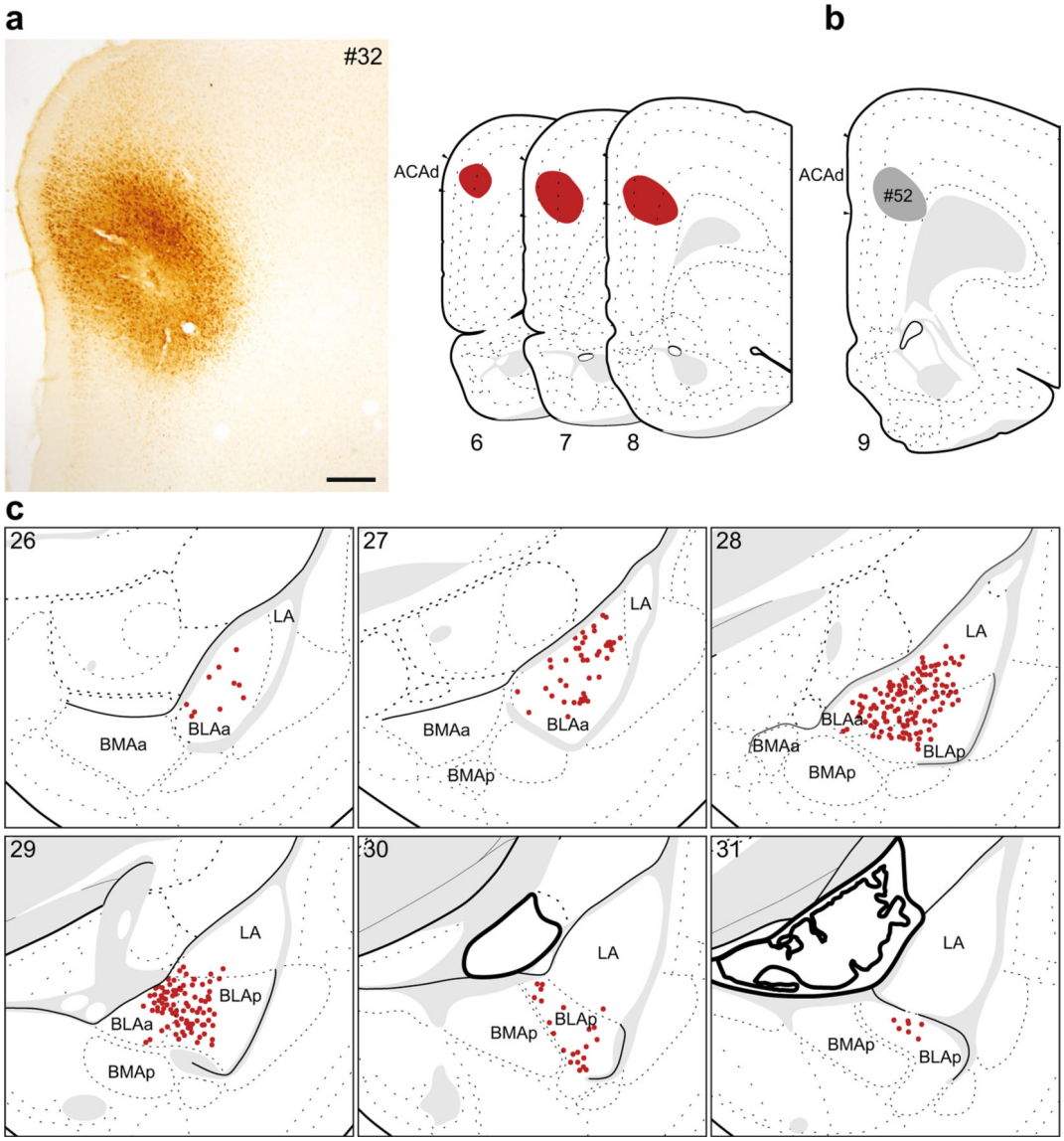

Fig. 2.

The distribution of labeling within the amygdala following retrograde tracer injection into the ACAd. **a** Photomicrograph of the injection center, and illustration of the rostrocaudal extent of the injection spread for case #32. **b** Illustration of injection center for a comparison injection into ACAd (#52). **c** Labeled neurons (*red dots*) were plotted onto rat brain templates derived from Swanson (2004), arranged from rostral to caudal. *Numbers* denote atlas levels, *scale bar* 200 μm

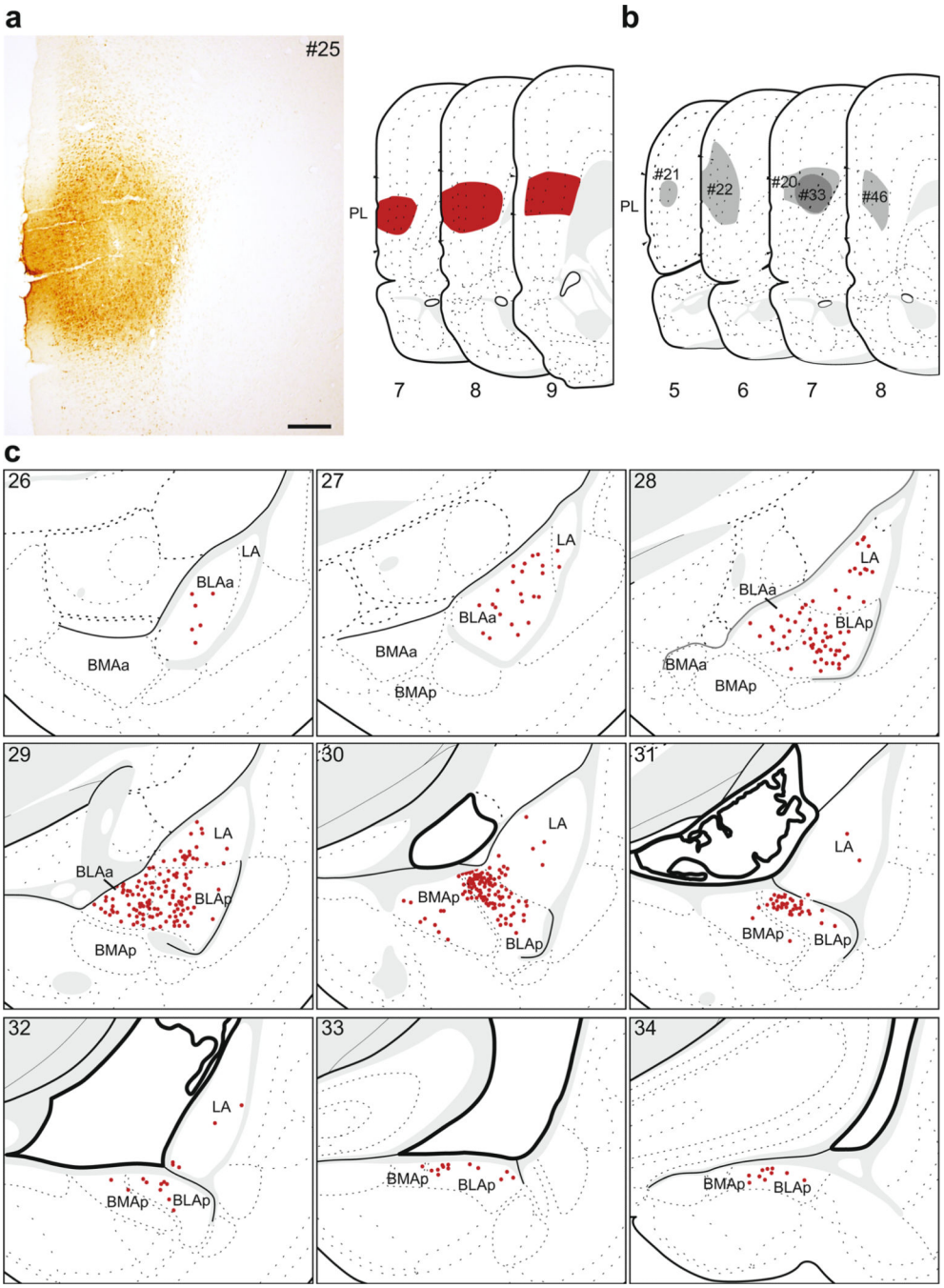

Fig. 3.

The distribution of labeling within the amygdala following retrograde tracer injection into PL. **a** Photomicrograph of the injection center, and illustration of the rostrocaudal extent of the injection spread for case #25. **b** Illustration of the injection centers for comparison injections into PL (#20–22, #33, #46). **c** Labeled neurons (*red dots*) were plotted onto rat brain templates derived from Swanson (2004), arranged from rostral to caudal. *Numbers* denote atlas levels, *scale bar* 200 μm

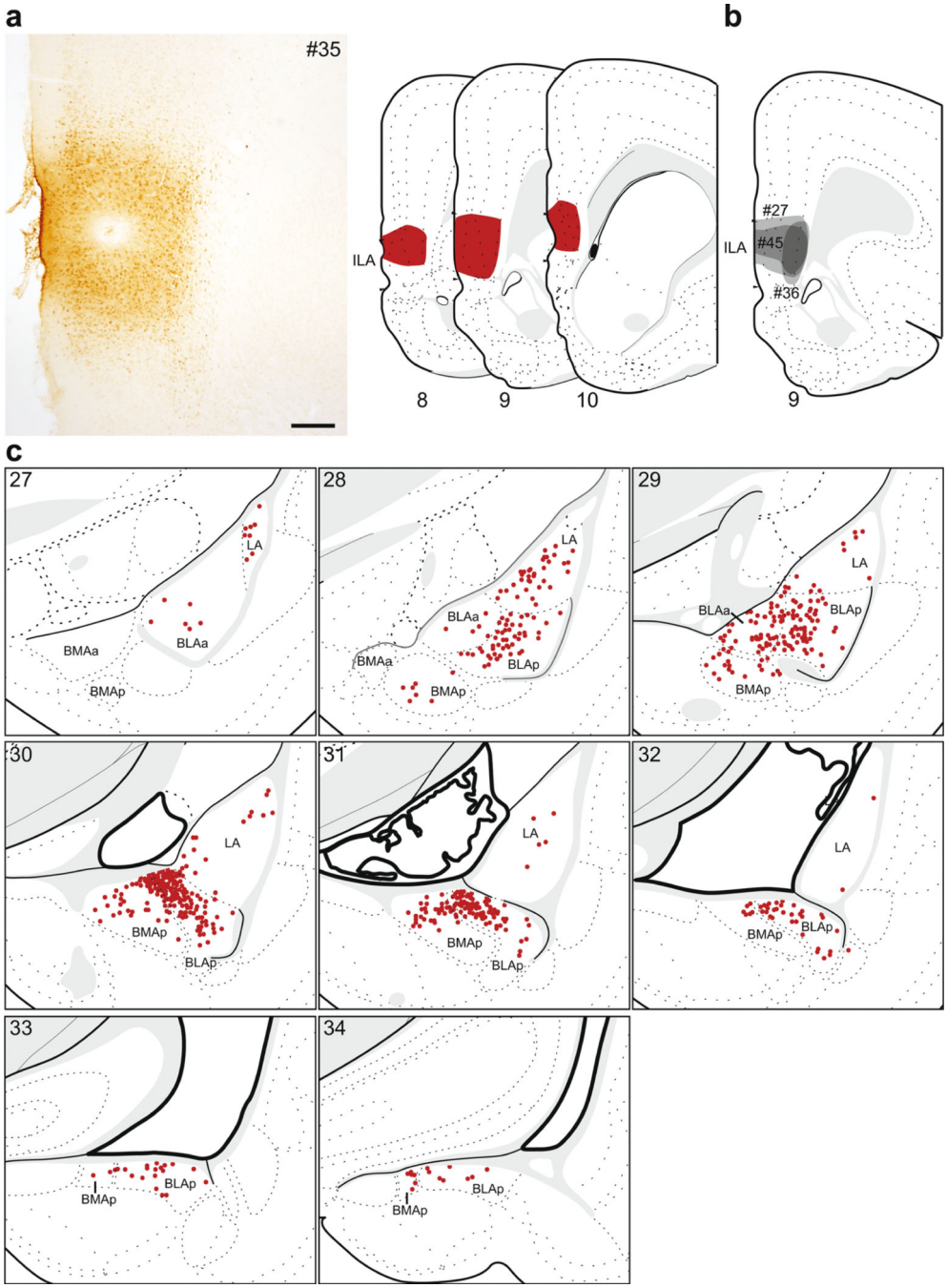

Fig. 4.

The distribution of labeling within the amygdala following retrograde tracer injection into ILA. **a** Photomicrograph of the injection center, and illustration of the rostrocaudal extent of the injection spread for case #35. **b** Illustration of the injection centers for comparison injections into ILA (#27, #36, #45). **c** Labeled neurons (*red dots*) were plotted onto rat brain templates derived from Swanson (2004), arranged from rostral to caudal. *Numbers* denote atlas levels, *scale bar* 200 μm

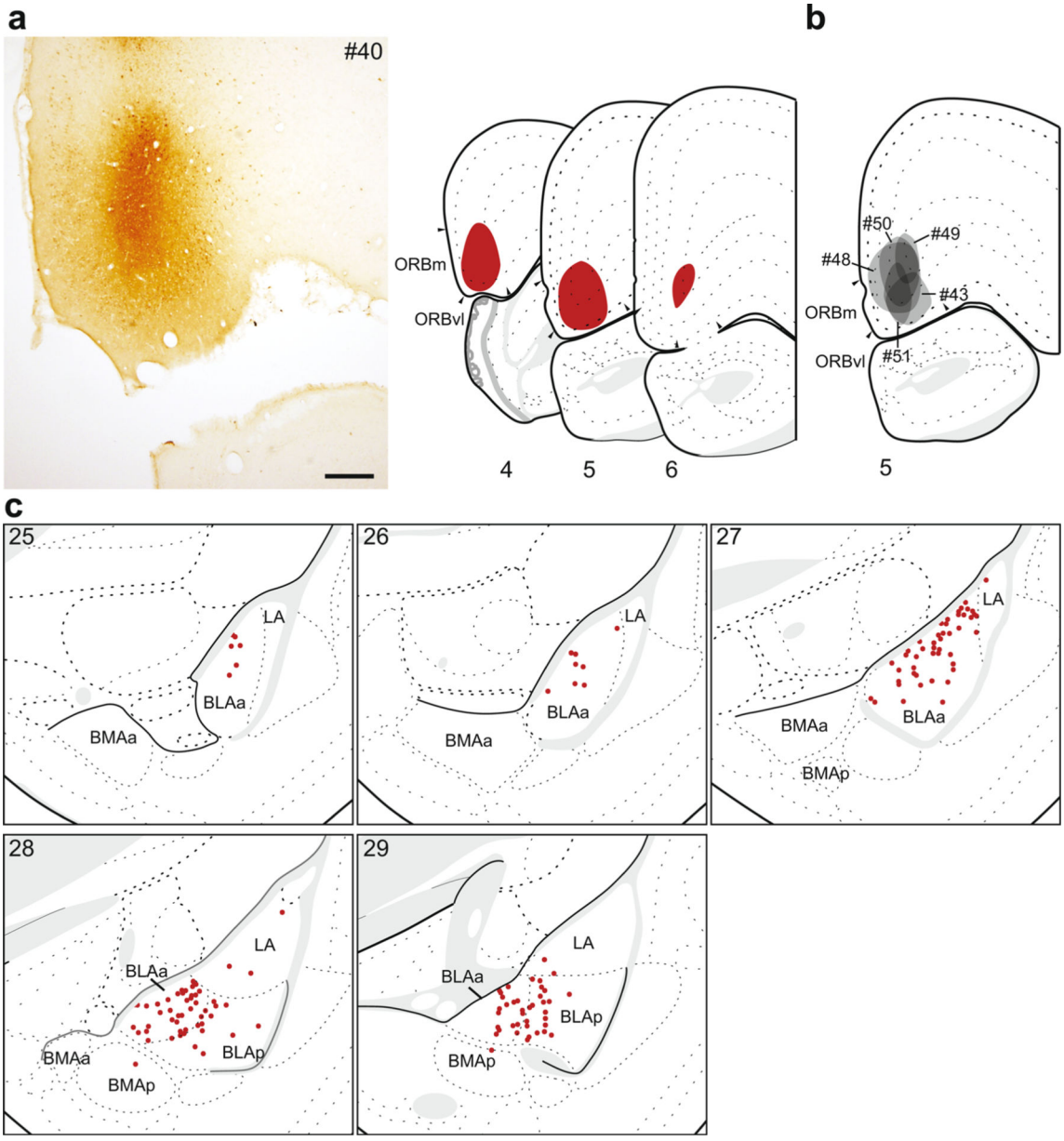

Fig. 5.

The distribution of labeling within the amygdala following retrograde tracer injection into rostromedial ORB (ORBm, vl). **a** Photomicrograph of the injection center, and illustration of the rostrocaudal extent of the injection spread for case #40. **b** Illustration of the injection centers for comparison injections into very rostral mPFC (#43, #48–51). **c** Labeled neurons (*red dots*) were plotted onto rat brain templates derived from Swanson (2004), arranged from rostral to caudal. *Numbers* denote atlas levels, *scale bar* 200 μm

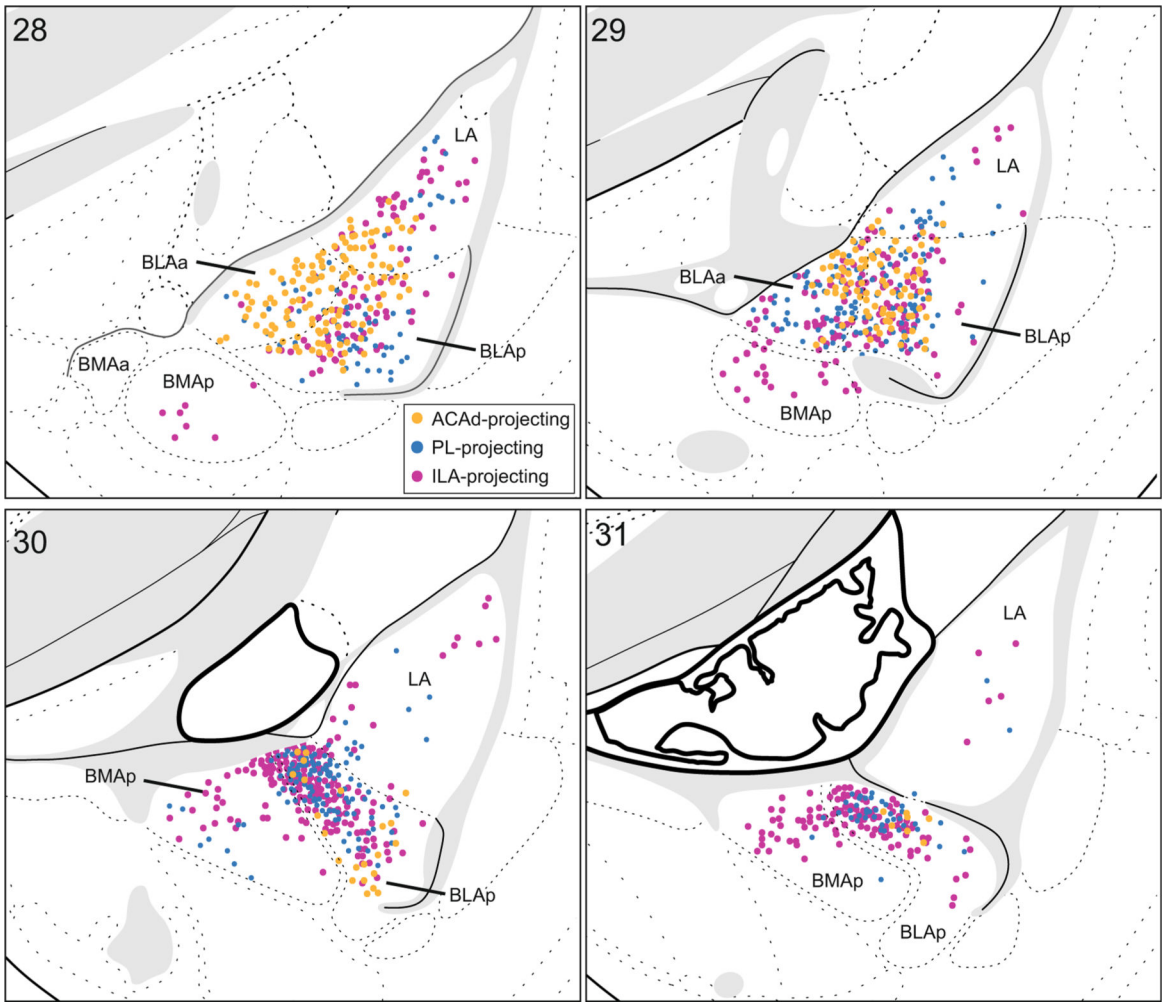

Fig. 6.

Topographical distribution of basolateral area projections to the mPFC. Combined labeling plots in the amygdala following ACAd (*orange*; from Fig. 2c), PL (*blue*; from Fig. 3c), and ILA (*pink*; from Fig. 4c) injections. Labeled neurons were plotted onto rat brain templates derived from Swanson (2004), arranged from rostral to caudal. *Numbers* denote atlas levels

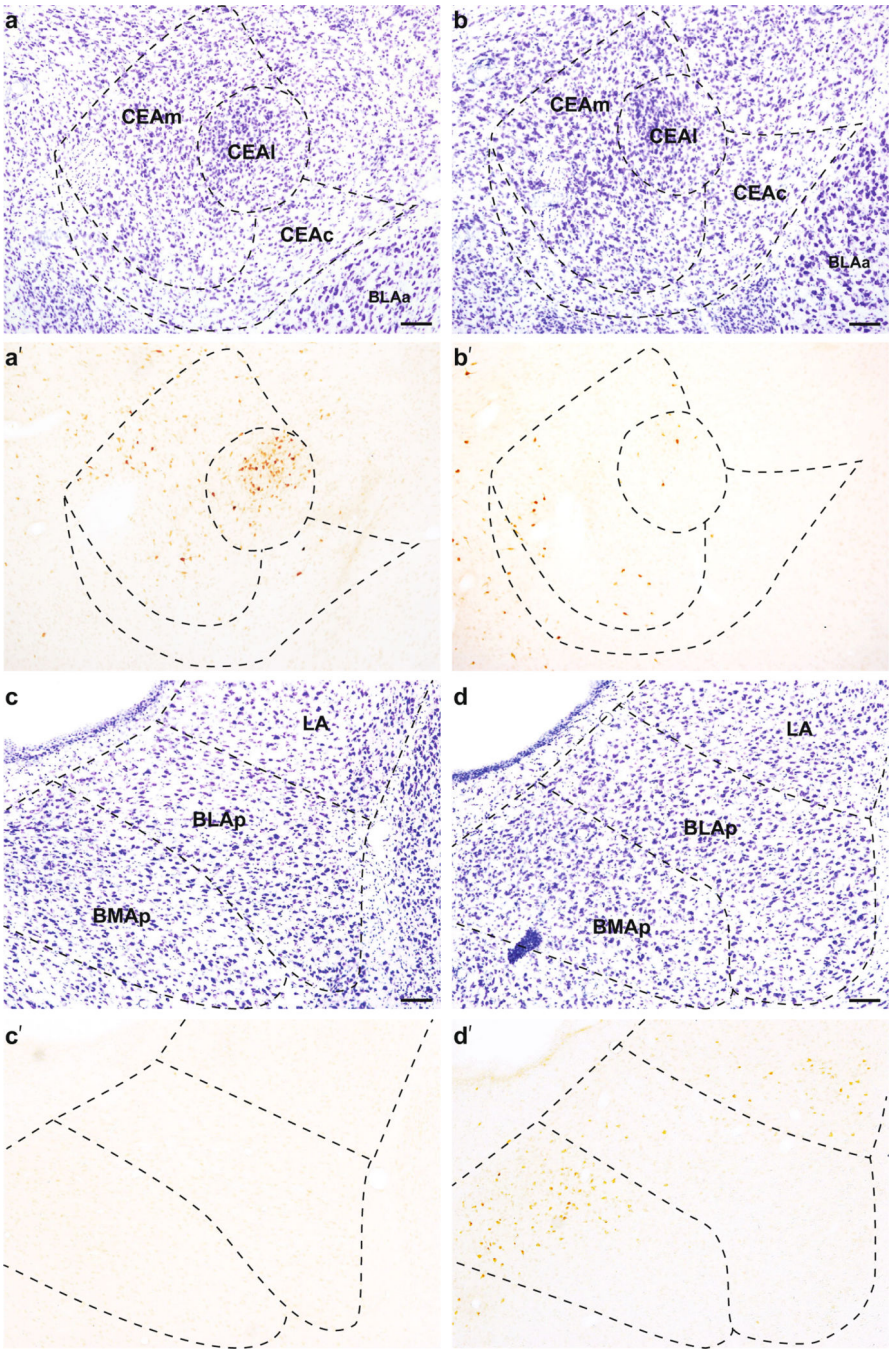

Fig. 7.

Representative images of retrograde tracer labeling in the amygdala; the CEA after tracer placement into dorsal (**a′**; #23) and ventral (**b′**; #21) LHA, and the basolateral area of the amygdala after tracer placement into dorsal (**c′**; #23) and ventral (**d′**; #21) LHA. **a**, **b** Adjacent Nissl-stained tissue. *Scale bars* 100 μm

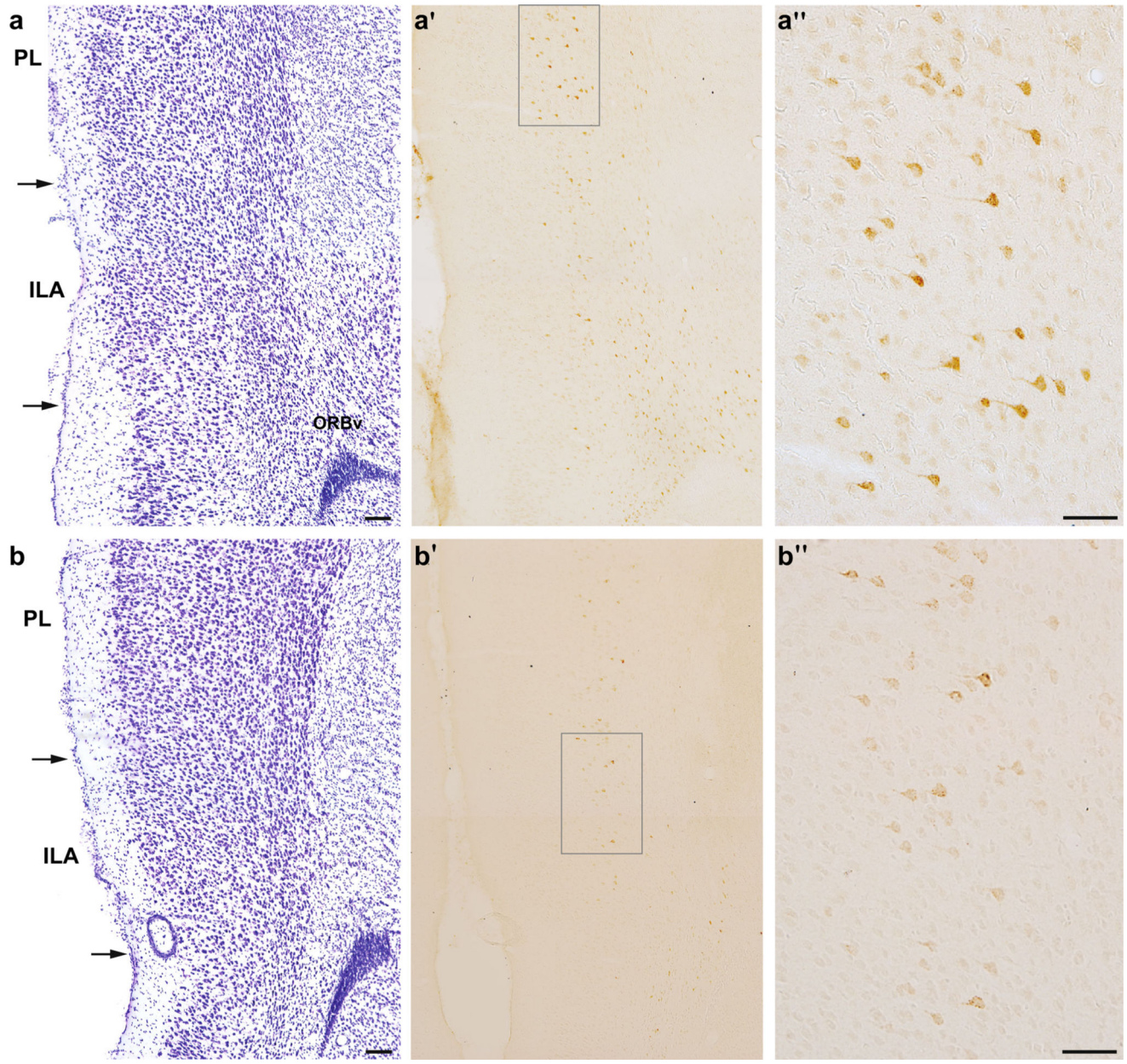

Fig. 8.

Photomicrographs show retrograde tracer labeling in the mPFC after tracer placement into dorsal (**a′**; #23) and ventral (**b′**; #24) LHA, and adjacent Nissl-stained tissue (**a**, **b**); *scale bars* 100 μm. Labeling within layer 5 after dorsal (**a″**) and ventral (**b″**) LHA, as indicated by *gray boxes* on **a′** and **b′**; *scale bars* 50 μm

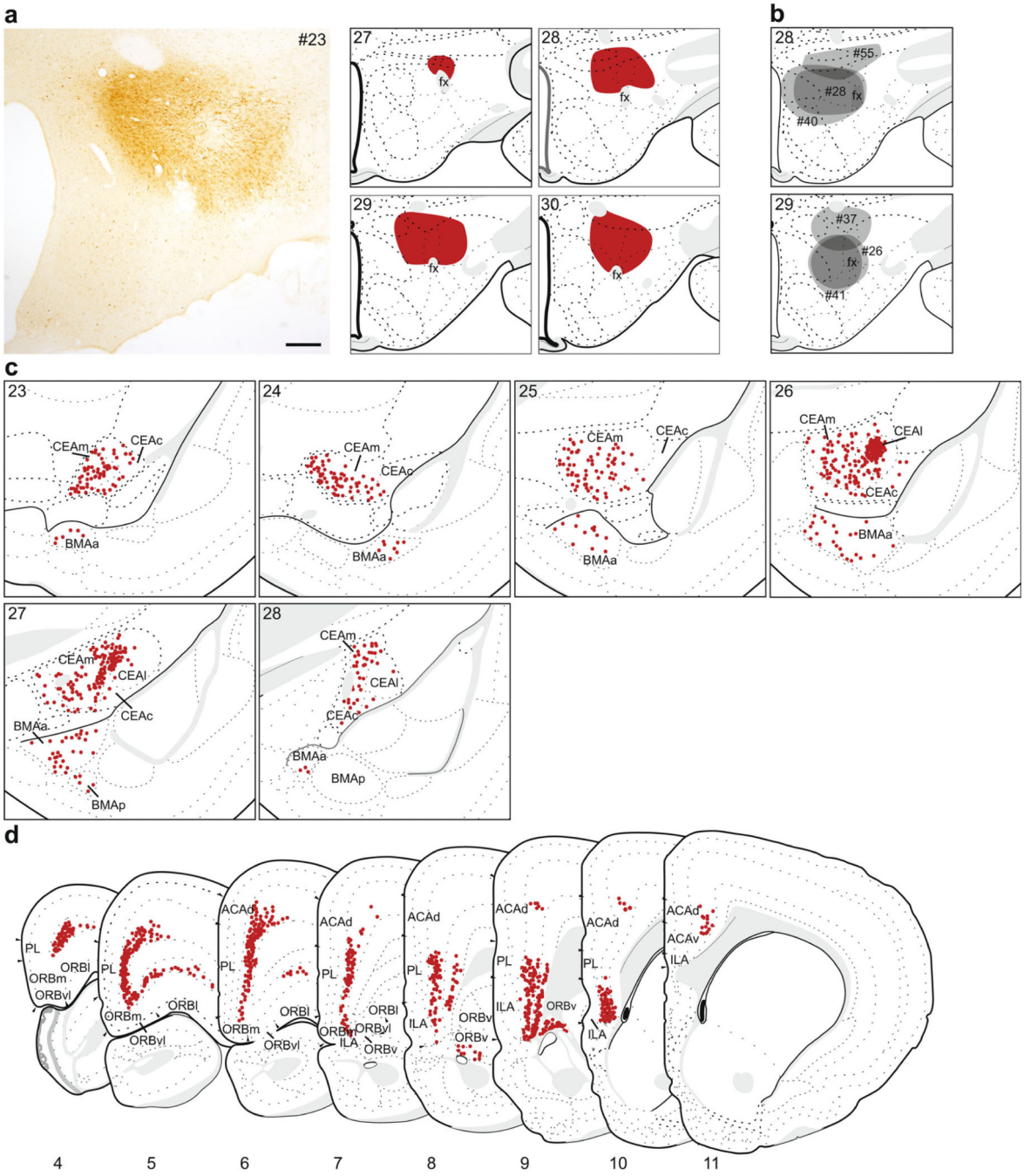

Fig. 9.

The distribution of labeling within the amygdala (**c**) and mPFC (**d**) following retrograde tracer injection into dorsal LHA. **a** Photomicrograph of the injection center, and illustration of the rostrocaudal extent of the injection spread for case #23. **b** Illustration of the centers of other injections into dorsal LHA (#26, #28, #37, #40, #41, #55). **c**, **d** Labeled neurons (*red dots*) were plotted onto rat brain templates derived from Swanson (2004), arranged from rostral to caudal. *Numbers* denote atlas levels, *scale bar* 200 μm

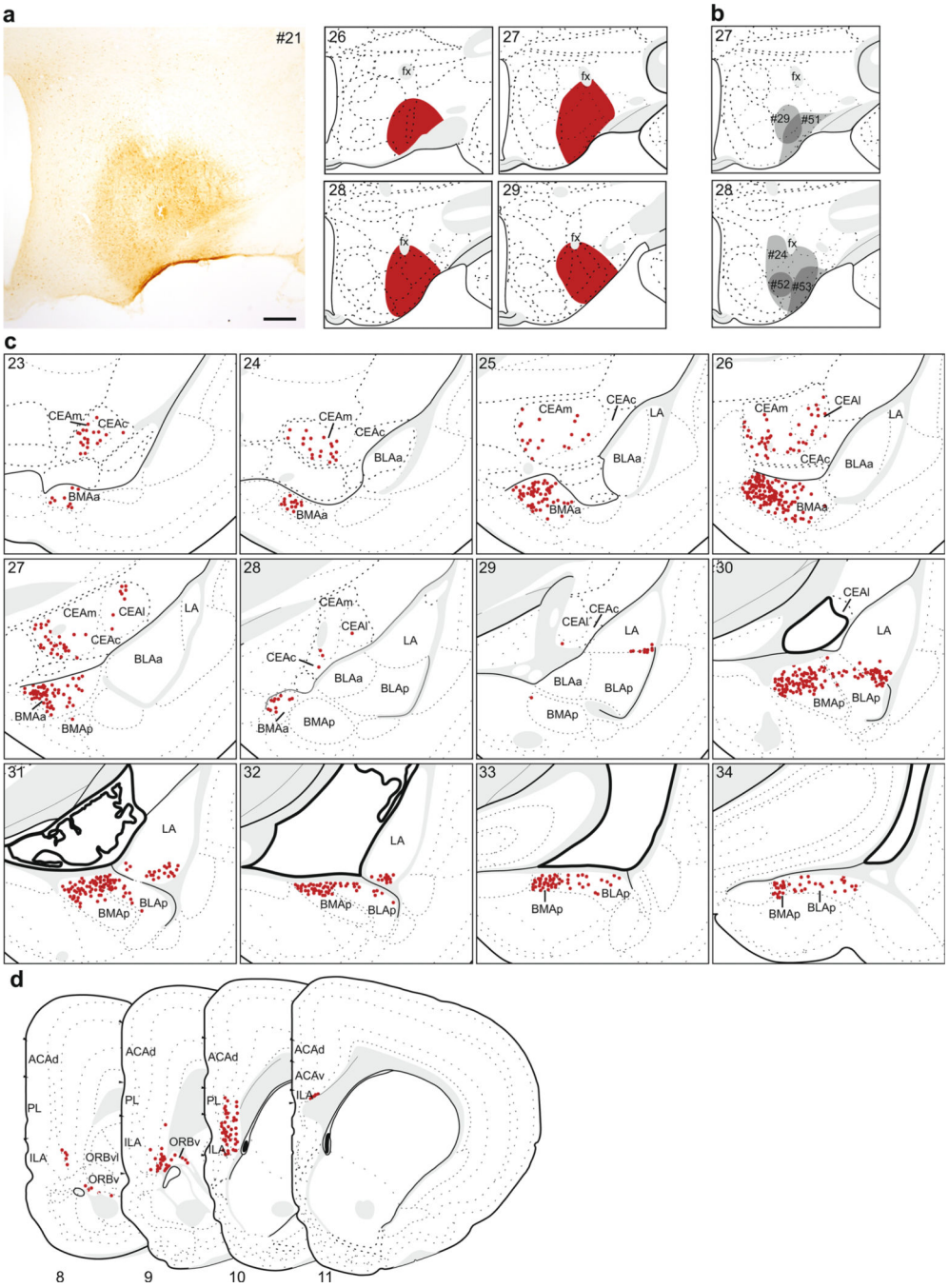

Fig. 10.

The distribution of labeling within the amygdala (**c**) and mPFC (**d**) following retrograde tracer injection into ventral LHA. **a** Photomicrograph of the injection center, and illustration of the rostrocaudal extent of the injection spread for case #21. **b** Illustration of the centers of other injections into ventral LHA (#24, #29, #51–53). **c**, **d** Labeled neurons (*red dots*) were plotted onto rat brain templates derived from Swanson (2004), arranged from rostral to caudal. *Numbers* denote atlas levels, *scale bar* 200 μm

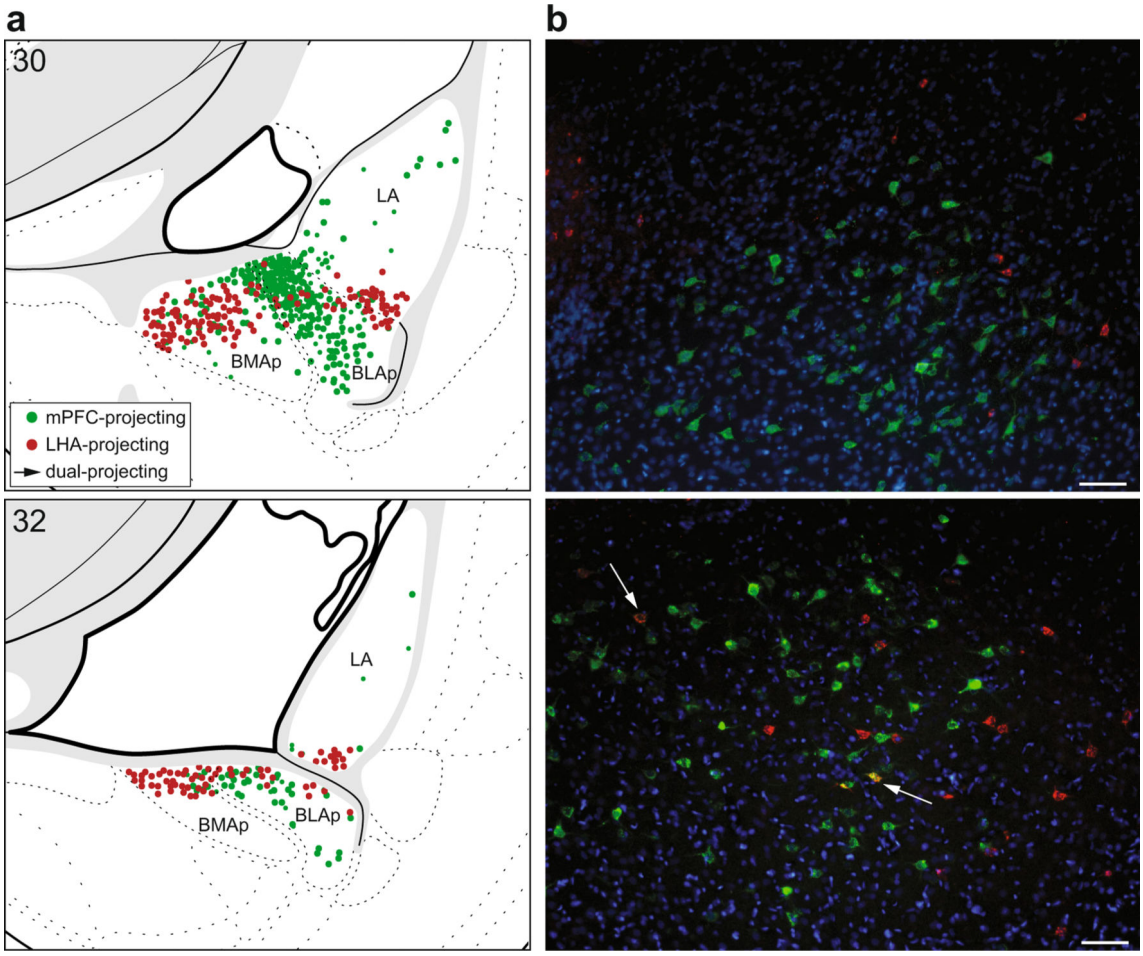

Fig. 11.

Distribution of mPFC-projecting (*green*) and LHA-projecting (*red*) neurons in the caudal basolateral area of the amygdala. **a** Illustration of total amygdala projections to all mPFC areas and both LHA regions (combined labeling plots from single-label analyses shown in Figs. 2c, 3c, 4c, 5c, 9c, and 10c). Labeled neurons were plotted onto rat brain templates derived from Swanson (2004); *numbers* denote atlas levels. **b** Representative images from a single brain used in the double-label analysis for simultaneous visualization of both tracers (case #20, injection in PL and a large injection in LHA). *Arrows* indicate double-labeled neurons which project to both the mPFC and LHA (*yellow*); *scale bars* 100 μm

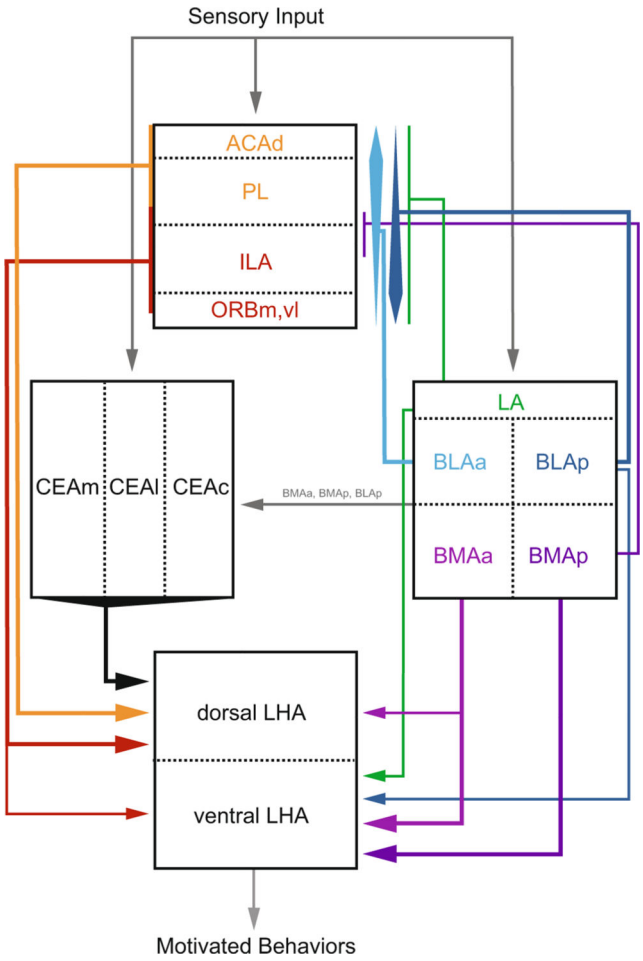

Fig. 12.

Summary of projections characterized in the present study. Selected other known projections are shown in *gray*

Table 1

Quantitative distribution of retrogradely labeled neurons within the amygdala following mPFC injections into the ACAd (#32), PL (#25), and ILA (#35)

	% by cell group				% by rostrocaudal location		
	BLAa	**BLAp**	**BMAp**	**LA**	**Rostral**	**Mid**	**Caudal**
ACAd	48.47	35.11	0.00	15.65	57.69	42.31	0.00
PL	19.21	60.84	7.39	12.56	20.69	69.46	9.85
ILA	8.72	59.93	18.00	13.36	18.18	66.79	15.03

For each mPFC target, shown are the percent of labeled neurons located within each cell group (there was no labeling in BMAa), and the percent of labeled neurons located within the rostral (atlas levels 26–28), mid (atlas level 29–31), and caudal (atlas levels 32–34) basolateral area (collapsed across cell groups)